HELICON WAVES IN A FLARING MAGNETIC FIELD

Part I: Equations in Spherical Coordinates and WKB-like Solutions

Donald Arnush and Arthur Peskoff

Electrical Engineering Department and
Biomathematics and Physiology Depts.

PPG-1538 March, 1995

Submitted to Plasma Physics and Controlled Fusion.

Helicon Waves in a Flaring Magnetic Field

Part I: Equations in Spherical Coordinates and WKB-like Wave Solutions

Donald Arnush* and **Arthur Peskoff†**

*Electrical Engineering Department
UCLA School of Engineering and Applied Science
Los Angeles, CA 90095-1594

†Departments of Biomathematics and Physiology
UCLA School of Medicine
Los Angeles, CA 90095-1766

Short Title: **Helicon Waves in a Flaring Magnetic Field**

Classification Numbers: 52.35.Hr

Abstract

Helicon waves (whistler waves bounded transversely by a magnetic field surface) occur in the ionosphere and are used in many industrial applications. Their propagation is investigated for a cylindrically symmetric curved (flaring) boundary using a finite element method where the propagation region is divided into a sequence of truncated cones. In each conical segment, the field lines are represented by a local spherical coordinate system whose origin is the apex of the cone. A vector wave equation for the fields is formulated for a cold plasma. It is reduced, in spherical coordinates, to a pair of coupled partial differential equations (PDEs) for two scalar functions. The PDEs are separable for the azimuthal eigenvalue $m = 0$. The separability conditions can be satisfied approximately for $m \neq 0$ for small cone angles far from the apex, and exactly only in the limit that the cone approaches a cylinder. It is shown that in this limit the solution approaches that for helicon waves in a cylinder. The θ-dependence is a Legendre function, with noninteger eigenvalues determined by the cone angle. The propagating solutions of the fourth-order ordinary differential equation, which describes the r-dependence, are obtained using a WKB-like method. When compared to the exact solutions found in Part II of this paper (Peskoff and Arnush 1995), the approximation is found to be excellent except near the apex of the cone. As an example of the use of conical functions for an arbitrarily flaring guide field, the WKB-like functions are used to calculate the propagation in a slowly diverging parabola of revolution.

I. Introduction

Low frequency electromagnetic whistler waves are well known in ionospheric and laboratory research. When transversely confined, they are often called "helicon" waves. They develop electrostatic components and their propagation and polarization characteristics are modified. An extensive review of the experimental and theoretical research on the properties of helicon waves confined to a cylinder was performed by Chen (1994). He discussed the unusually high plasma production efficiency, uniformity, and quiescence of helicon plasma sources, and their consequent suitability for semiconductor processing and other industrial applications.

In both ionospheric and industrial cases, helicon waves are usually confined to regions bounded by curved static magnetic field ($\mathbf{B}_0$) line surfaces. Yet, while theoretical and experimental treatments of cylindrically confined helicon waves are a vigorous ongoing research subject, there is very little experimental or theoretical published research (aside from *ad hoc* WKB treatments) on helicon waves confined in a nonuniform field geometry. In this paper, we will consider that case by first formulating a vector wave equation for an arbitrary $\mathbf{B}_0$. We anticipate calculating the propagation in an axisymmetric guide field by employing a method (see, e.g., Sporleder and Unger 1979, or Solymar 1959) commonly used for calculating microwave propagation in horns and couplers. For guided waves in vacuum, authors usually segment the enclosed region into either a sequence of cylinders, or a sequence of lenticular regions with coaxial conical sides and spherical surfaces perpendicular to the axis. In this paper, where a plasma-filled guide is considered, we anticipate a choice of the latter approach, using spherical coordinates in each region with the origins at the apexes of the cones. The magnetic field lines then coincide with radius vectors on the conical surfaces and the axis, and are well approximated by them in between. The bulk of this paper is devoted to analyzing the fields in the cones. The helicon vector wave equation is reduced to a pair of coupled equations for two scalar functions, and general solutions to the field equations are found. Examining the boundary conditions at the conical surfaces, we find that the coupled equations are not separable in spherical coordinates except for azimuthally symmetric waves ($m = 0$ mode), or for the small cone angle limit ($r \to \infty$ with $r\vartheta$ fixed, i.e. the limit that the cones approach cylinders) and arbitrary m. The relationship between conically and cylindrically confined cases are discussed in some detail. The equations are then considered for the intermediate frequency case

$$\omega_{ci} \ll \omega \ll \omega_{ce} \ll \omega_{pe} \quad , \tag{1}$$

where ω, ω_c and ω_p are the wave, cyclotron, and plasma frequencies, respectively, and i and e refer to ions and electrons. A WKB-like solution is obtained which is useful except in a small range of r near $r = 0$. It is used to calculate helicon wave propagation in a parabola of revolution. In the following paper (Peskoff and Arnush 1995, hereinafter referred to as II), solutions of the fourth order ODE valid everywhere are obtained. The solutions involve convergent expansions about the origin, and asymptotic expansions about infinity with overlapping ranges of validity. They are joined using a double integral representation.

II. Vector Wave Equation

We form an orthogonal curvilinear coordinate system ξ_1, ξ_2, ξ_3, where $\hat{\boldsymbol{\xi}}_3$, the unit vector along ξ_3, coincides with the magnetic field line (i.e., $\mathbf{B}_0 = B_0 \hat{\boldsymbol{\xi}}_3$). Assuming $\exp(-i\omega t)$ time dependence, most of the dominant physical properties of helicon waves can be obtained using the dielectric tensor for a cold collisional plasma (see e.g. Stix 1992),

$$\varepsilon = \begin{vmatrix} S & -iD & O \\ iD & S & 0 \\ 0 & 0 & P \end{vmatrix} \quad , \tag{2}$$

where the three tensor directions at any point coincide with the three orthogonal curvilinear coordinates, and

$$S = \frac{1}{2}(R+L) = 1 - \sum_j \frac{\omega_{pj}^2}{\omega^2 - \omega_{cj}^2} \quad , \tag{3a}$$

$$D = \frac{1}{2}(R-L) = \sum_j \frac{\varepsilon_j \omega_{cj} \omega_{pj}^2}{\omega\left(\omega^2 - \omega_{cj}^2\right)} \quad , \tag{3b}$$

$$P = 1 - \sum_j \frac{\omega_{pj}^2}{\omega^2} \quad , \tag{3c}$$

where, in the usual manner, j is the species and ε_j the sign of its charge. Landau damping cannot be included in this dielectric formulation, except in an *ad hoc* way, because we do not Fourier transform the equations along the direction of wave propagation. Using equations (2), (3), and Maxwell's equations, we readily obtain

$$\nabla \times \mathbf{B} / \mu_0 = \mathbf{J} - i\omega\varepsilon_0 \mathbf{E} = -i\omega\varepsilon_0 \left[S\,\mathbf{E}_\perp + P E_3 \hat{\boldsymbol{\xi}}_3 + iD\hat{\boldsymbol{\xi}}_3 \times \mathbf{E} \right] \quad , \tag{4}$$

where $\mathbf{E}_\perp = \mathbf{E} - E_3\hat{\boldsymbol{\xi}}_3$. Equation (4) can be inverted to solve for $\mathbf{E}$ in terms of $\nabla \times \mathbf{B}$. Using $i\omega\mathbf{B} = \nabla \times \mathbf{E}$, we obtain

$$k_0^2\mathbf{B} = \nabla \times \left[i\beta_1\hat{\boldsymbol{\xi}}_3 \times (\nabla \times \mathbf{B}) - \beta_2(\nabla \times \mathbf{B}) + \beta_3(\nabla \times \mathbf{B})_3\hat{\boldsymbol{\xi}}_3\right] \tag{5}$$

where

$$\begin{aligned} k_0 &= \frac{\omega}{c} \quad , \quad \beta_1 = \frac{L-R}{2RL} = \frac{D}{D^2-S^2} \quad , \\ \beta_2 &= -\frac{R+L}{2RL} = \frac{S}{D^2-S^2} \quad \text{and} \quad \beta_3 = \frac{1}{P} + \beta_2 \end{aligned} \quad . \tag{6}$$

The terms multiplying β_1, β_2, and β_3 in equation (5) are primarily due to Hall current, displacement current, and a balance between displacement and polarization currents, respectively. In vacuum, $\beta_1 = \beta_3 = 0$, $\beta_2 = -1$, and equation (5) reduces to the vector Helmholtz equation $(\nabla^2\mathbf{B} + k_0^2\mathbf{B} = 0)$. For intermediate frequencies typical of laboratory values $(n_0 = 10^{13}\text{cm}^{-3}$, $B_0 = 1\,\text{kG}$ and $\omega/2\pi = 27\,\text{MHz})$, the inequalities in equation (1) obtain, and

$$\beta_1 \cong \frac{\omega\,\omega_{ce}}{\omega_{pe}^2} \cong 10^{-4}, \quad \beta_2 \cong \frac{\omega}{\omega_{ce}}\beta_1, \quad \text{and} \quad \beta_3 \cong \beta_2 \quad .$$

Hence, $\beta_1 \gg \beta_2 \gg \beta_3$. At higher frequencies, in the $\omega \to \omega_{ce}$ limit, β_2 approaches β_1 but β_3 remains negligible.

III. Vector Equation Separation in Spherical Coordinates

We employ the multipolar potential method, used by Morse and Feshback (1953) to separate the vector Helmholtz equation in five confocal quadratic coordinate systems, by applying it to equation (5) in spherical coordinates and assuming that

$$\mathbf{B} = \mathbf{M} + \mathbf{N}, \qquad \mathbf{M} = \nabla \times (\hat{\mathbf{r}}\,r\psi), \qquad \text{and} \qquad \mathbf{N} = \nabla \times \nabla \times (\hat{\mathbf{r}}\,r\chi) \quad . \tag{7}$$

Since $\hat{\mathbf{r}} \cdot \mathbf{M} = 0$ and $\mathbf{r} \cdot \nabla \times \mathbf{N} = 0$, $\mathbf{M}$ and $\mathbf{N}$ are interpreted as transverse magnetic and transverse electric fields, respectively. For the vector Helmholtz equation, $\mathbf{M}$ and $\mathbf{N}$ and hence ψ and χ are decoupled, and each scalar function satisfies the scalar Helmholtz equation, e.g., $\nabla^2\psi + k_0^2\psi = 0$. For the helicon wave equation, we insert equation (7) into equation (5), and find that $\mathbf{M}$ and $\mathbf{N}$ are coupled. The insertion yields an equation of the form

$$\nabla \times \mathbf{P}(\psi, \chi, \hat{\mathbf{r}}) = 0 \quad ,$$

$$\mathbf{P} = \left[i\beta_i \hat{\mathbf{r}} \times (\nabla \times \mathbf{B}) - \beta_2 (\nabla \times \mathbf{B}) + \beta_3 \hat{\mathbf{r}} \cdot (\nabla \times \mathbf{B}) \hat{\mathbf{r}} \right] - k_0^2 \left[\hat{\mathbf{r}} r\psi + \nabla \times (\hat{\mathbf{r}} r\chi) \right] \tag{8}$$

Equation (8) is solved if we can demonstrate that there exists a function, f, such that

$$\mathbf{P}(\psi, \chi, \hat{\mathbf{r}}) = -\nabla f \quad . \tag{9}$$

Equating the vector components of equation (9), we find that it is satisfied for

$$f = i\beta_1 r \nabla^2 \chi + \beta_2 \frac{\partial}{\partial r}(r\psi) \quad .$$

Using this relation to eliminate f from the component equations, we obtain

$$k_0^2 r\psi = \frac{\partial}{\partial r}\left(i\beta_1 r\nabla^2 \chi\right) + \beta_2 r\nabla^2 \psi + \frac{d\beta_2}{dr}\frac{\partial}{\partial r}(r\psi) - \beta_3 \left[r\nabla^2 \psi - \frac{\partial^2}{\partial r^2}(r\psi) \right] , \tag{10a}$$

$$k_0^2 r\chi = i\beta_1 \frac{\partial}{\partial r}(r\psi) + \beta_2 r\nabla^2 \chi \quad . \tag{10b}$$

The β_1, β_2, and β_3, and hence the plasma parameters, may be functions of r, but not θ or ϕ. In the intermediate frequency approximation of equation (1) this condition requires that n_0/B_o be a function of r only. Thus, in contrast to the usual treatments of cylindrically confined waves in which exponential z dependence of the fields is assumed from the start, the equation is separable for plasma parameter variation along, but not transverse to, the direction of wave propagation. Since ϑ and φ derivatives in equations (10a) and (10b) appear only as ∇^2, we expand ψ and χ in the angular eigenfunctions of ∇^2, the spherical harmonics $Y_{\ell,m}(\vartheta, \varphi) = P_\ell^m(\cos\vartheta)\exp(im\varphi)$, where $P_\ell^m(\cos\vartheta)$ is the Legendre function:

$$r\psi = \sum_{\ell,m} F_{\ell,m}(r) Y_{\ell,m}(\vartheta, \varphi) \quad \text{and} \quad r\chi = \sum_{\ell,m} G_{\ell,m}(r) Y_{\ell,m}(\vartheta, \varphi) \quad . \tag{11}$$

The separation constants ℓ and m are determined by the boundary conditions. Since $0 \leq \varphi < 2\pi$, and the fields are continuous, m is an integer and the m-modes are independent. Defining the operator D_ℓ^2

$$D_\ell^2 = \frac{d^2}{dr^2} - \frac{\ell(\ell+1)}{r^2} \quad , \tag{12}$$

inserting equation (11) in equations (10), using the second order differential equations that $\exp(i\,m\,\varphi)$ and $P_\ell^m(\cos\theta)$ satisfy, and the orthogonality of the $\exp(i\,m\,\varphi)$ to eliminate the sum over m, we obtain

$$\sum_\ell \left\{ k_0^2\,F_{\ell,m} - \beta_2\,D_\ell^2\,F_{\ell,m} - \beta_2'\,F'_{\ell,m} - \beta_3\,\frac{\ell(\ell+1)}{r^2}\,F_{\ell,m} - \left(i\beta_1\,D_\ell^2\,G_{\ell,m}\right)' \right\} P_\ell^m \;=\; 0 \qquad (13a)$$

$$\sum_\ell \left\{ k_0^2\,G_{\ell,m} - \beta_2\,D_\ell^2\,G_{\ell,m} + i\beta_1\,F'_{\ell,m} \right\} P_\ell^m \;=\; 0 \quad , \qquad (13b)$$

where the primes denote differentiation with respect to r. We assume an insulating boundary. Then for each m, the component of the current perpendicular to the boundary, J_ϑ, vanishes. Using equations (4),(5),(7), and (11), we obtain at the conical boundary

$$\mu_0\,r J_\vartheta \;=\; \sum_\ell \Bigg\{ \left[(1+\beta_2)\,\frac{d}{d\theta}\,P_\ell^m \;-\; \frac{m}{\sin\vartheta}\,\beta_1\,P_\ell^m \right] F'_{\ell,m} \;+$$

$$+\; i\left[\beta_1\,\frac{d}{d\theta}\,P_\ell^m - (1+\beta_2)\,\frac{m}{\sin\vartheta}\,P_\ell^m \right] D_\ell^2\,G_{\ell,m} \Bigg\} \Bigg|_{\vartheta=\vartheta_0} \;=\; 0 \quad , \qquad (14)$$

For separability, it is required that there exist a set of eigenvalues of ℓ, such that for each eigenvalue, the curly-bracketed expression in the boundary condition (14) vanishes for all r. For these eigenvalues of ℓ, the $P_\ell^m(\cos\theta)$ would then be an orthogonal set of eigenfunctions. As a consequence of the orthogonality, the expressions in curly brackets in equations (13a) and (13b), for each ℓ, must vanish, leading to a pair of coupled differential equations for $F_{\ell,m}$ and $G_{\ell,m}$. The expression in curly brackets in equation (14) does not separate into a function of r times a function of θ, unless $F_{\ell,m}/D_\ell^2\,G_{\ell,m}$ is independent of r. But this can be seen to be impossible if $F_{\ell,m}$ and $G_{\ell,m}$ are solutions of the coupled differential equations arising from equations (13). (The functions F and G would be over-prescribed: three nonredundant equations for two unknown functions). Thus, separability can occur only if both expressions in square brackets in equation (14) vanish simultaneously for all r. This is in turn possible if either

$$\beta_1 = 1+\beta_2 \qquad \text{and} \qquad \left[\frac{d}{d\theta}\,P_\ell^m(\cos\theta) \;-\; \frac{m}{\sin\theta}\,P_\ell^m(\cos\theta) \right] \Bigg|_{\theta=\theta_0} \;=\; 0 \qquad (15a)$$

or $$m = 0 \qquad \text{and} \qquad \frac{d}{d\theta}\,P_\ell^m(\cos\theta)\Big|_{\theta=\theta_0} \;=\; 0 \qquad (15b)$$

are satisfied. The condition $\beta_1 = 1 + \beta_2$ in equation (15a) is not physically realizable for the intermediate frequency case equation (1). Consequently, separability is only achievable for the azimuthally symmetric case $m = 0$. In effect, the transverse electric and magnetic modes satisfy functionally different conditions at the boundary, and their coupling by the helicon interaction prevents the general simultaneous satisfaction of both. (For fixed ℓ, in the large r limit, G_ℓ/r^2 can be neglected, F'_ℓ and G''_ℓ approach proportionality and hence the equation can be satisfied approximately for each ℓ. The point is well illustrated in figure (1), which shows the normalized magnitude and phase of $F'_\ell \,/\, D^2_\ell\, G$ for an outgoing wave, computed from the solutions developed in II, for β_1 constant and $\beta_2 = \beta_3 = 0$. The result might be anticipated from the fact that for large r and fixed $r\theta_0$, a conical segment approaches a segment of a cylinder in which higher order modes are separable.) For further insights from comparison with the cylindrical case, including a generalization of the familiar helicon dispersion relation of Chen (1992), see Appendix A. Unlike the case where $P^m_\ell(\cos\theta)$ covers the domain of $0 \le \vartheta \le \pi$, the eigenvalues, ℓ, are not integers if $\vartheta_0 \neq \pi$. Finding a spectrum of ℓ values which satisfy equation (14) for $m > 0$ is beyond the scope of this work. The goal of the remainder of this effort is to analyze the axisymmetric case $m = 0$.

Setting $m = 0$, and using the orthogonality of the P_ℓ in equations (13), we obtain

$$k_0^2\, F_\ell - \beta_2\, D^2_\ell\, F_\ell - \beta'_2\, F'_\ell - \beta_3\, \frac{\ell(\ell+1)}{r^2}\, F_\ell - \left(i\,\beta_1\, D^2_\ell\, G_\ell\right)' \;=\; 0 \qquad \text{(13c)}$$

$$k_0^2\, G_\ell - \beta_2\, D^2_\ell\, G_\ell + i\,\beta_1\, F'_\ell \;=\; 0 \quad . \qquad \text{(13d)}$$

IV. Intermediate Frequency m = 0 Waves

We now proceed to investigate the solutions to equations (13c) and (13d) in the intermediate frequency regime of equation (1) for $m = 0$. Neglecting β_1 and β_2, defining the function $H_\ell = D^2_\ell\, G_\ell$, and eliminating $F_\ell = i\,\beta_1\, H'_\ell/k_0^2$, equations (13c) and (13d) can be reduced to the single equation

$$\frac{d^2}{dr^2}\left[\beta_1\,\frac{d^2}{dr^2}\,(\beta_1\, H_\ell)\right] \;-\; \frac{\ell(\ell+1)}{r^2}\,\beta_1\,\frac{d^2}{dr^2}\,(\beta_1\, H_\ell) - k_0^4\, H_\ell \;=\; 0 \quad . \qquad (16)$$

To explore the solutions to equation (16), we follow Chen (1992) and assume, for the sake of simplicity, that there is no plasma production and negligible transverse plasma transport in the flaring field. In that case, we expect that $\beta_1 \propto B_0/n_0$ will be constant. Defining

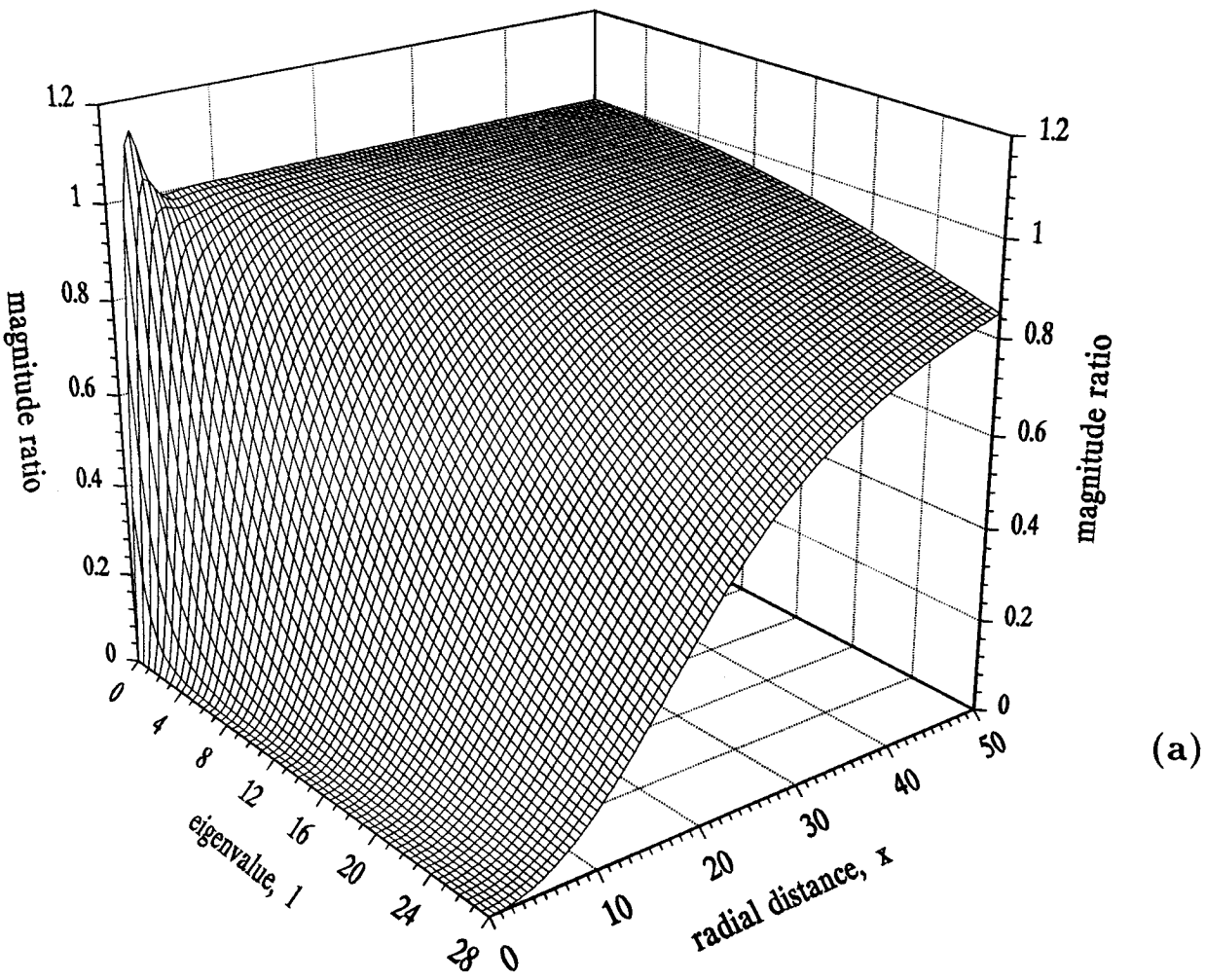

Figure 1: Comparison of G_ℓ and H_ℓ as a function of ℓ and $x = qr$ for $\beta_1 = k_0^2/q^2$ constant and $\beta_2 = \beta_3 = 0$: **(a)** magnitude of $G_\ell \,/\, H_\ell \;\propto\; F_\ell' \,/\, (D_\ell^2\, G_\ell)$; and **(b)** phase of H_ℓ minus phase of G_ℓ.

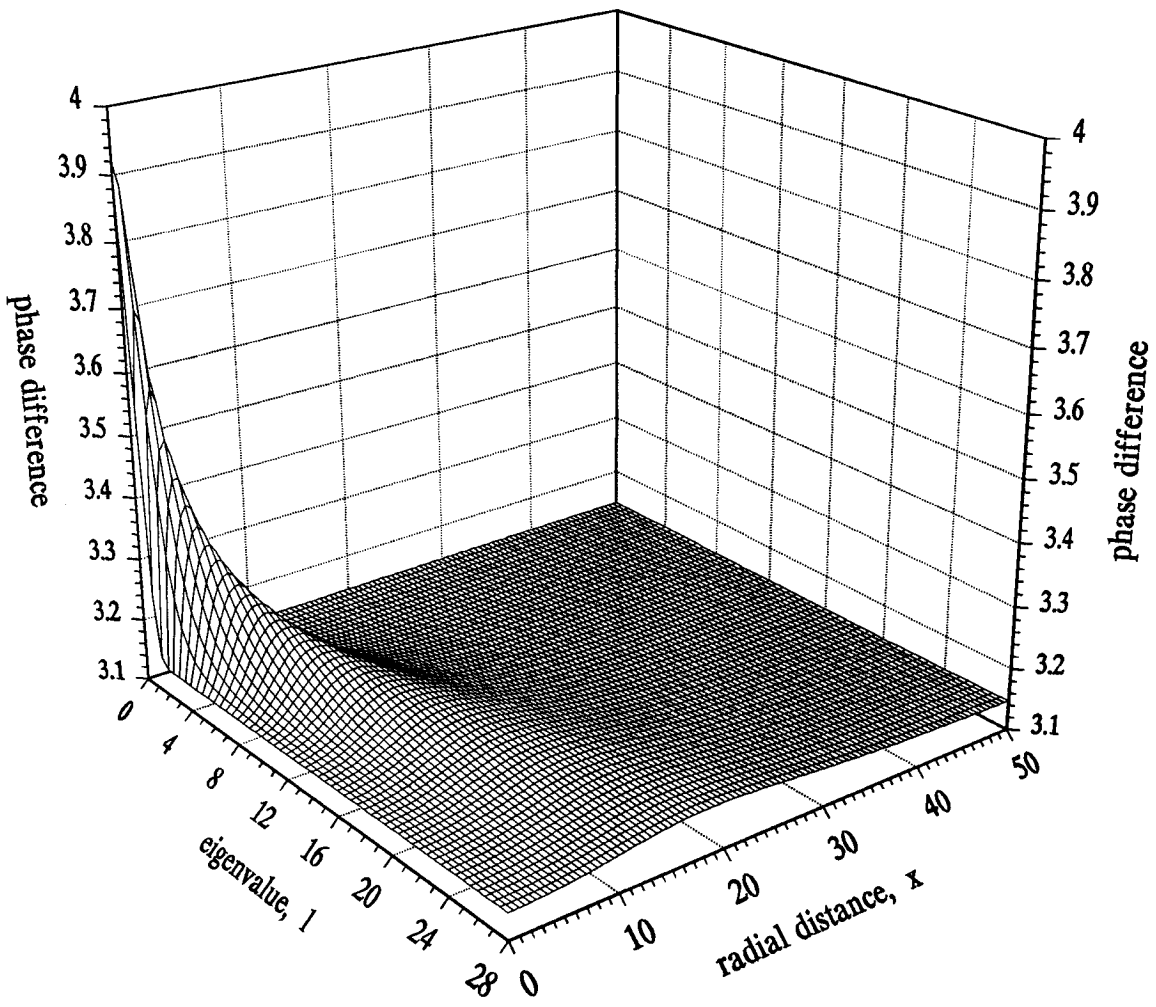
phase difference
4
3.9
3.8
3.7
3.6
3.5
3.4
3.3
3.2
3.1
0
4
8
12
16
20
24
28
eigenvalue, l
0
10
20
30
40
50
radial distance, x
phase difference

(b)

$q^2 = k_0^2/\beta_1$ and $x = qr$, where $q = k_0/\beta_1^{1/2}$ is the whistler wave number in an unbounded medium, equation (16) takes the deceptively simple form

$$\frac{d^4}{dx^4} H_\ell - \frac{\ell(\ell+1)}{x^2} \frac{d^2}{dx^2} H_\ell - H_\ell = 0 \quad . \tag{17}$$

The fields take on a simple form in terms of H:

$$\begin{aligned} \mathbf{B}_{\ell,0} &= \hat{\mathbf{r}} \frac{\ell(\ell+1)}{x^2} P_\ell H_\ell'' + \frac{1}{x} P_\ell' \left(\hat{\boldsymbol{\vartheta}} H_\ell''' - i\hat{\boldsymbol{\varphi}} H_\ell' \right) \\ \mathbf{E}_{\ell,0} &= \frac{\omega}{qx} P_\ell' \left(\hat{\boldsymbol{\vartheta}} H_\ell - i\hat{\boldsymbol{\varphi}} H_\ell'' \right) \quad . \end{aligned} \tag{18}$$

For fixed ℓ, in the limit $x \to \infty$ the second term in equation (17) becomes negligible, and the four independent solutions to the equation take the form $\exp(p_i\, x)$, where the p_i are the four roots of one, corresponding to outgoing and incoming waves, and growing and decaying exponentials. To further describe the fields, we exploit the connection between small angle cones and cylinders. The fact that the second order differential equation for the Legendre function in the small angle approximation, $\sin\vartheta \approx \vartheta$, becomes Bessel's equation, provides an approximation to P_ℓ which is accurate to about 1% in finding the zeros of P_ℓ' at $\vartheta_0 = 1\,(n \approx 3)$, and improves for larger n. For:

$$J_0' = -J_1(j_{1,n}) = 0\,, \qquad P_\ell(\cos\vartheta) \cong J_0\left(\left[\ell + \tfrac{1}{2}\right]\vartheta\right)\,, \qquad \ell_n \cong \frac{j_{1,n}}{\vartheta_0} - \tfrac{1}{2} \quad . \tag{19}$$

Noting Appendix A, equation (15'b), for $r \sim a/\vartheta_0$ we have $\ell/x \sim (j_{1,n}/\vartheta_0)\,(\vartheta_0/a/q) \sim T/q$, showing directly the correspondence between the cone and cylinder equations and eigenvalues.

Obtaining propagating solutions of the stiff equation (17) by straight-foward numerical integration is complicated by the presence of exponentially growing solutions which amplify the numerical noise. In the following paper (Peskoff and Arnush 1995), we solve (17) by developing power series expansions about $x = 0$ for the four independent solutions. We then develop asymptotic series for the outgoing and incoming waves, as well as the growing and decaying exponential solutions, which can represent the solution for large x. These two sets of solutions are then connected, using a double-integral representation valid for all x. In this paper, using a WKB approach, a simple function is found that represents the two propagating waves accurately except for small x.

V. WKB-like Solution to Equation (17)

A WKB-like solution to equation (17) can be obtained by assuming the form

$$H(x) \;=\; A(x)\exp\Big(i\,\phi(x)\Big) \;=\; A(x)\,\exp\Big(i\int_{x_0}^{x} k(y)\,dy\Big) \quad , \tag{20}$$

where x_0 is an arbitrary location where the phase is chosen to be zero. $A(x)$ and $k(x)$ are assumed to be slowly varying functions, so that we can neglect (using a prime to denote derivative with respect to x) A'', k'', $k'\,A'$, and $(k')^2$, with respect to A, k, A' and k'. Inserting equation (20) in equation (17) and requiring that both the real and imaginary parts of the equation be satisfied, we get

$$k^4 \,+\, U^2\,k^2 \,-\, 1 \;=\; 0 \quad , \tag{21}$$

$$2k\left(2k^2 \,+\, U^2\right)A' \,+\, \left(6k^2 \,+\, U^2\right)k'\,A \;=\; 0 \quad , \tag{22}$$

where $U^2(x) = \ell(\ell+1)\,/\,x^2$ corresponds to T^2 in the cylindrical case. We choose the propagating roots of equation (21):

$$k(x) \;=\; \pm\,\Big[\,\tfrac{1}{2}\Big(\sqrt{U^4(x)+4}\;\;-\,U^2(x)\Big)\,\Big]^{1/2} \quad . \tag{23}$$

Differentiating equation (21) and inserting the result in equation (22), we get

$$\frac{k'}{k} \;=\; -\,\frac{1}{2\,(2k^2+U^2)^2}\,\frac{dU^2}{dx}$$

$$\frac{A'}{A} \;=\; \tfrac{1}{4}\,\frac{6k^2+U^2}{(2k^2+U^2)^2}\,\frac{dU^2}{dx} \;=\; \tfrac{1}{4}\,\frac{3\sqrt{U^4+4}\,-2U^2}{U^4+4}\,\frac{dU^2}{dx} \quad , \tag{24}$$

which can be integrated exactly to yield

$$A(x) \;=\; \frac{\Big[U^2(x)\,+\,\sqrt{U^4(x)+4}\,\Big]^{3/4}}{\Big[\,2\Big(\,U^4(x)+4\,\Big)\,\Big]^{1/4}} \quad . \tag{25}$$

Thus, the form of equation (20) with the phase obtained from equation (23) are analogous to the WKB solution of a second order equation. However, the amplitude differs significantly from the second order result, $A = 1/(k)^{1/2}$.

It is convenient, particularly in view of the exact solutions obtained in II, to fix the phase of the WKB-like approximation so that

$$\phi(x) \;=\; \int_{x_0}^{x} k(y)\,dy \;=\; x + I(x) \quad ,$$

where $I(x)$ vanishes at infinity. Taking x_0 arbitrarily large, subtracting the arbitrarily large constant, and changing variables, we obtain

$$\phi(x) = x + \frac{\sqrt{\ell(\ell+0)}}{2} \int_0^{U(x)} \frac{dy}{y^{3/2}} \left\{ 1 - \left[\frac{\sqrt{x^2+4} - x}{2} \right]^{1/2} \right\}$$

$$\underset{x \to \infty}{\longrightarrow} x \left[1 + \frac{1}{4} U(x) - \frac{1}{96} U^2(x) - \frac{1}{160} U^3(x) + \ldots \right] \quad . \tag{26}$$

Thus, the WKB-like approximation provides an excellent bridge to the cylindrical limit $x \to \infty$, $U(x) \to T$.

The condition $k \gg k'/k$ is well satisfied for $\ell \gtrsim 5$ for

$$x \gtrsim \ell^{2/3} \quad . \tag{27}$$

We borrow from II to display, as a function of x and ℓ, the ratio of the WKB-like to the exact amplitude in figure (2a), and the difference between the WKB-like and exact phases in figure (2b). The contour plot projections shown at the bottom of the figures illustrate the fact that the WKB-like approximation is excellent for many cases of physical interest.

The fields in this approximation are given by equations (17) and (18) with

$$\frac{H'}{H} = i\,k - \frac{6k^2 + U^2}{U^4 + 4} \left(\frac{U^2}{2x} \right) \quad ,$$

$$\frac{H''}{H} = -k^2 \left[1 + i\,\frac{4k}{x}\,\frac{U^2}{U^4+4} \right] \quad ,$$

$$\frac{H'''}{H} = -i\,k^3 + \tfrac{3}{2}\,\frac{k^2\,U^2}{x}\,\frac{2k^2 - U^2}{U^4+4} \tag{28}$$

VI. Propagation in a Slowly Flaring Guide Field

We calculate the propagation of helicon waves in a guide field of arbitrary axisymmetric shape by approximating the guide by a sequence of finite elements, each of which is a lenticular truncated cone (with spherical base and cap), as described in the introduction. Each element defines a spherical coordinate system centered at the apex of the cone. The cone angle θ_0 determines the eigenvalues ℓ, and the field solution in each element is given by the above analysis for the helicon wave in a conical region. We may pass to the limit of infinitesimal element thickness to treat a field shape exactly. For concreteness, consider

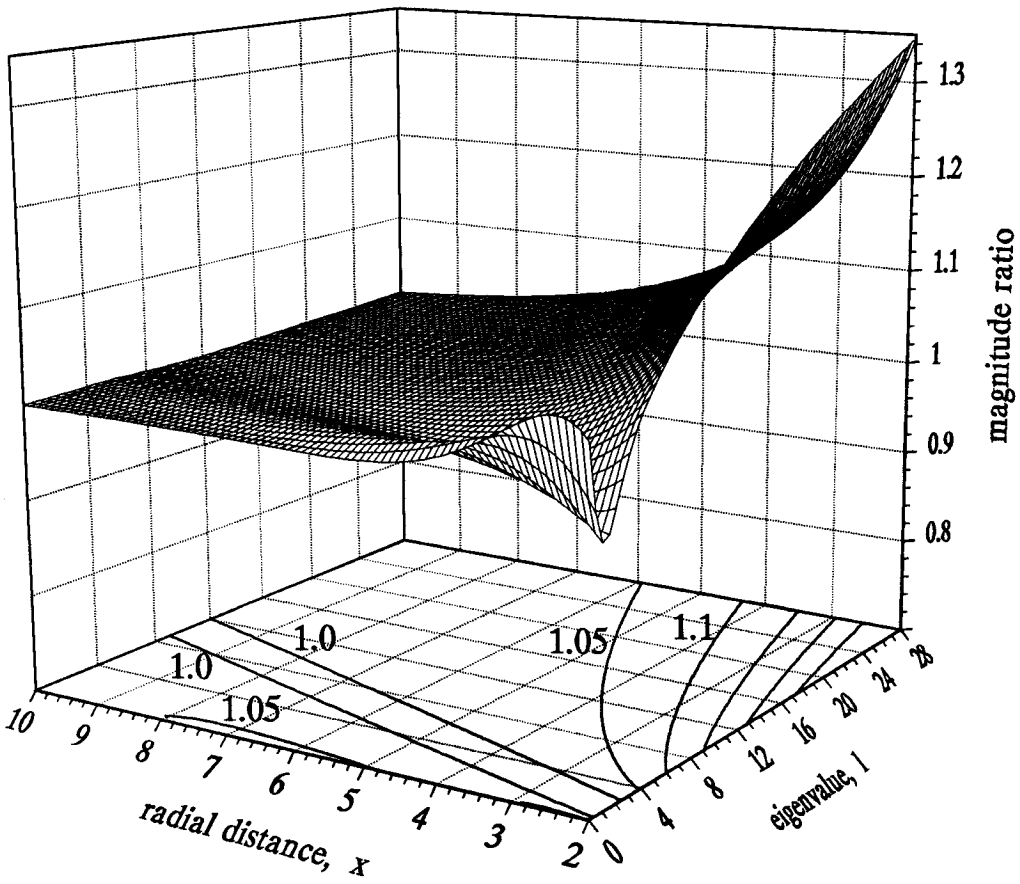

(a)

Figure 2: (a) The ratio of the magnitude of the WKB-like to exact solutions. Contours of constant ratio are shown at the bottom. (b) The difference between the WKB-like and exact solution phases. Constant phase difference contours are shown at the bottom.

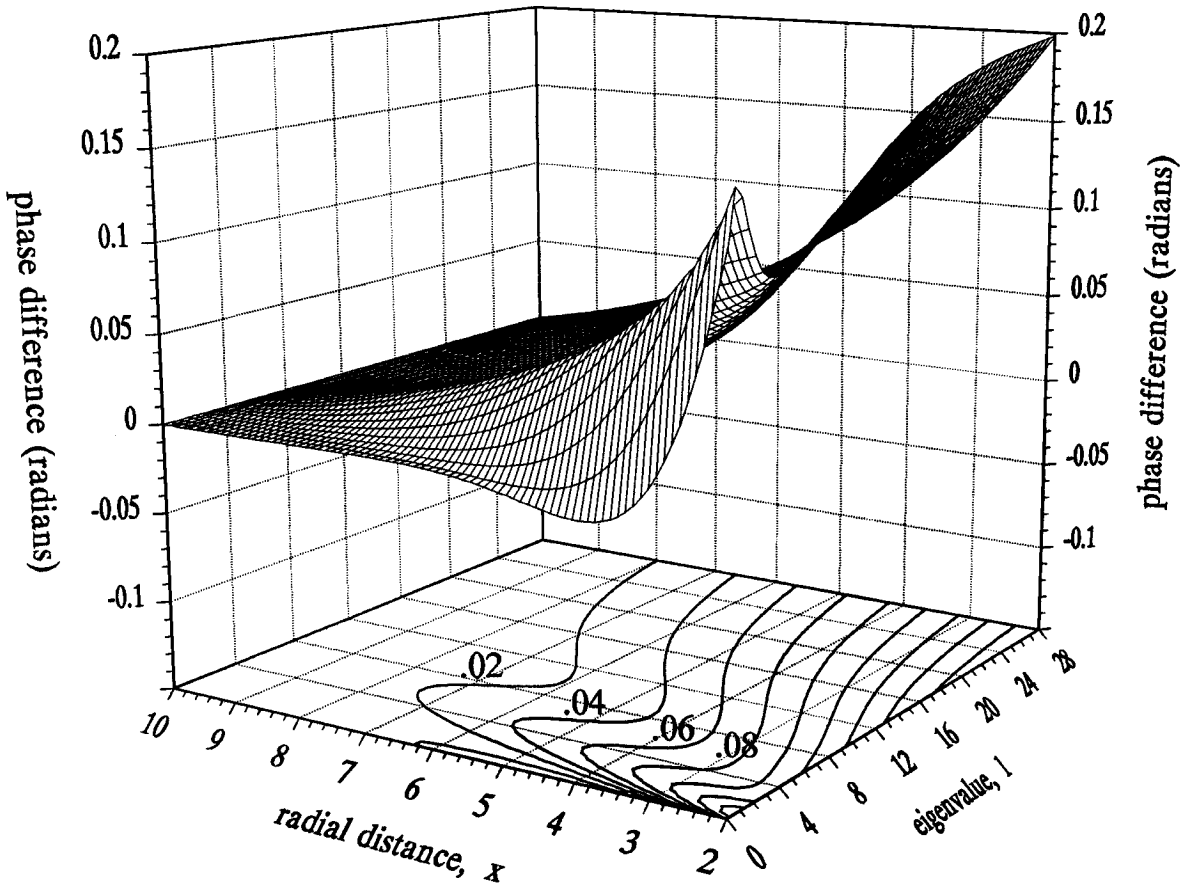
0.2
0.15
0.1
0.05
0
-0.05
-0.1
phase difference (radians)
0.2
0.15
0.1
0.05
0
-0.05
-0.1
phase difference (radians)
.02
.04
.06
.08
10
9
8
7
6
5
4
3
2
0
radial distance, x
4
8
12
16
20
24
28
eigenvalue, l

(b)

figure (3), where we index each truncated conical element by the z-coordinate of its left-hand boundary circle. Consider a wave incident at $z = 0$ from a cylindrical guide on the left. Conical waves propagate from element to element, with all components of their vector fields continuous at the spherical interfaces. At the spherical surface separating regions n and $n+1$, to insure that the fields be continuous as a function of ϑ, the field solution of the n region is expanded in spherical harmonics of the $n+1$ region in the well established manner. Thus, a spectrum of ℓ-modes is generated. Consider a single order ℓ-mode (the order corresponding to the order of the solution to equation (15)). To insure field continuity in the radial direction, H_ℓ, H'_ℓ, H''_ℓ, and H'''_ℓ must be continuous and, in the general case, all four solutions of equation (17) have to be employed. For $z \leq 0$ (in the cylinder) we have an incident and a reflected wave, and a solution which decreases exponentially to the left. In the interior elements, we have all four solutions. If there are N interfacial surfaces, in element $N+1$, which includes the point at infinity, we have an outgoing wave and a wave that decreases exponentially to the right. For a unit incident wave, there are 4 N functions and 4 N equations corresponding to the conditions at the surfaces. If we terminate the eigenfunction series at L, it is necessary to solve 4 LN simultaneous equations in 4 LN unknowns. In this section, as an illustration of the properties of the conical helicon functions, we investigate the case of propagation of the fundamental ℓ-mode in a parabolically flaring field, where the flare is sufficiently gradual for the influence of reflected and exponential waves and higher ℓ-mode generation to be negligible.

Let $h(\ell, x)$ be the outgoing wave solution in a cone, normalized to unit amplitude at $x = \infty$, and the solution throughout the bounded region be $H(z)$. In any element, the ℓ value will be fixed and x will vary. Let the ℓ value be identified by the z value at the left-hand surface. Thus, in region 1, where $z_0 < z < z_1$, we have for $H(z_0) = 1$:

$$H(z) \;=\; \frac{h\,[\,\ell\,(z_0)\,,\,x(z)\,]}{h\,[\,\ell\,(z_0)\,,\,x\,(z_0)]} \quad . \tag{29}$$

Define the quantities

$$H_n \;=\; H\,(z_n) \qquad \text{and} \qquad h_{m,n} \;=\; h\,[\,\ell\,(z_m)\,,\,x\,(z_n)\,] \quad . \tag{30}$$

Hence, $H_1 \;=\; h_{0,1} \,/\, h_{0,0}$. In region 2, where $z_1 < z < z_2$,

$$H(z) \;=\; H_1\,\frac{h\,[\,\ell\,(z_1)\,,\,x(z)\,]}{h\,[\,\ell\,(z_1)\,,\,x\,(z_1)]} \quad , \tag{31}$$

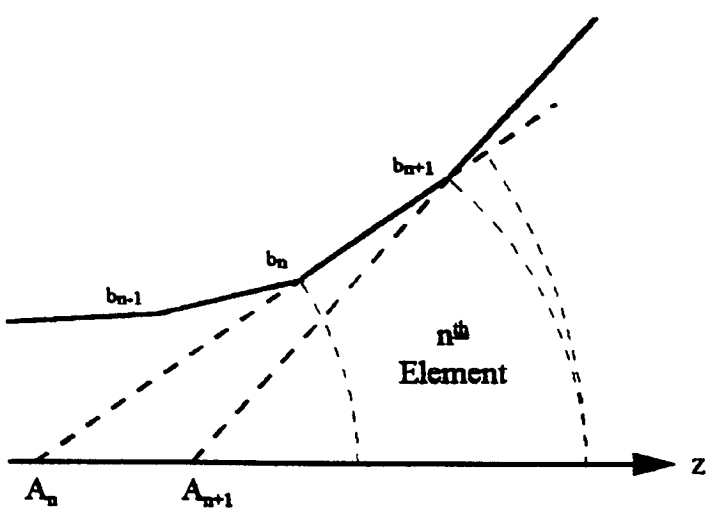

Figure 3: Construction of a finite element (conical segmentation) in flaring fields. In a plane which includes the axis of symmetry, z, boundary points b_n are selected at uniform z-coordinate intervals (for example). A_n is the intersection of the z-axis and the line which includes b_n and b_{n+1}. The nth conical segment is bounded by the cone with its apex at A_n, and the spherical surfaces with centers at A_n and radii given by the distances (A_n, b_n) and $(A_n, A_{n+1}) + (A_{n+1}, b_{n+1})$.

and

$$H_2 \;=\; H_1 \,\frac{h_{1,2}}{h_{1,1}} \;=\; \frac{h_{0,1}}{h_{0,0}}\;\frac{h_{1,2}}{h_{1,1}} \quad . \tag{32}$$

By induction, we have

$$H\,(z_{n+1}) \;=\; H_{n+1} \;=\; H_n\,\frac{h_{n,n+1}}{h_{n,n}} \;=\; \prod_{j=0}^{n}\;\frac{h\,[\,\ell\,(z_j)\,,\,x\,(z_{j+1})]}{h\,[\,\ell\,(z_j)\,,\,x\,(z_j)\,]} \quad . \tag{33}$$

Equation (31) is the basis of the numerical calculation to follow. It is of interest to write this result analytically, by passing to the limit of infinitesimal truncated cones. From equation (33), we have

$$\frac{H_{n+1}-H_n}{H_n} \;=\; \frac{h_{n,\,n+1}-h_{n,n}}{h_{n,n}} \quad , \tag{34}$$

which we rewrite as

$$\frac{1}{H}\;\frac{\Delta H}{\Delta z} \;=\; \frac{1}{h}\;\frac{\Delta_x h}{\Delta x}\;\frac{\Delta x}{\Delta z}\,\Bigg|_{\ell=\,\text{constant}} \quad . \tag{35}$$

If the tangent angle of the bounding curve is ϑ, then in the infinitesimal limit $dx\,/\,dz \;=\; \cos\vartheta$, and we have

$$\ell n\left[\,H(z)\,\right] \;=\; \int_0^z dz'\,\left[\,\cos\vartheta\,(z')\;\frac{\partial}{\partial x}\;\ln\left\{\,h(\ell,x)\,\right\}\,\right]\Bigg|_{\ell=\ell(z'),\,x=x(z')} \quad . \tag{36}$$

Propagation was calculated for helicon waves incident from the left at $z = 0$ into a region where the bounding magnetic field lines form a parabola of revolution with a cylindrical radius

$$\rho(z) \;=\; a\left(1 \,+\, z^2\,/\,b^2\right) \quad . \tag{37}$$

Reflections and higher order ℓ-mode coupling were neglected, and the WKB-like approximation, equation (20), was used for the propagating cone function $h(\ell,\,x)$. The plasma parameters were characterized using

$$\sigma \;=\; 10^{-10}\;\frac{n}{B}\;\mathrm{cm}^{-3}\,G^{-1} \quad , \tag{38}$$

and $\omega/2\pi = 27$ MHz. For comparison with "typical" parameters for a plasma processing tool (A. Chambrier of Plasma Materials Technologies (PMT), Inc., private communication), B_z was calculated on the axis $(\theta = 0)$ for $a = 4\,\mathrm{cm}$, $b = 10\,\mathrm{cm}$, and $\sigma = 0.5,\,1,\,2$, as shown in figure (4a). Similar calculations using the exact functions of II yield essentially identical results. The apparent "wavelength" (distance between the first two zero crossings) varies inversely with σ and the fields diminish rapidly, in qualitative agreement with PMT results. The variation with field geometry (i.e., the parameters a and b) are shown in figures

4b, c, and d. Figure (4d) approximates the case of a cylinder ($b \gg a$) and reproduces the anticipated result that the waves are sinusoidal with the wavelength nearly inversely proportional to σ. The geometric variations for fixed $\sigma = 1$ are summarized in figure (5).

Acknowledgment

The authors thank Professor F.F. Chen for suggesting this problem and for many helpful discussions.

APPENDIX A: Helicon Waves in a Cylinder

Eliminating F from equations (12) yields a fourth order differential equation for G, with four independent solutions. To analyze equation (13) further, it is instructive to consider propagation in a cylinder using the multipolar potential formulation. In that case, use equation (7) with the substitution $\hat{\mathbf{r}}\, r \rightarrow \hat{\mathbf{z}}$. The separation proceeds as in equations (8) and (9), resulting in equations (10′), with the derivatives with respect to z rather than r, and the factor r everywhere replaced by 1:

$$k_0^2\,\psi \;=\; \frac{\partial}{\partial z}\left(i\beta_1\,\nabla^2\chi\right) + \beta_2\,\nabla^2\psi + \frac{d\beta_2}{dz}\,\frac{\partial\psi}{\partial z} - \beta_3\left[\nabla^2\psi - \frac{\partial^2\psi}{\partial z^2}\right] \quad , \qquad (10'\text{a})$$

$$k_0^2\,\chi \;=\; -i\,\beta_1\,\frac{\partial\psi}{\partial z} + \beta_2\,\nabla^2\chi \quad . \qquad (10'\text{b})$$

To expand in eigenfunctions, use in place of equation (11)

$$\psi \;=\; \sum_{T,m} F_{T,m}(z)\,J_m(T\rho)\,\exp(im\varphi) \quad \text{and} \quad \chi \;=\; \sum_{T,m} G_{T,m}(z)\,J_m(T\rho)\,\exp(im\varphi) \quad , \qquad (11')$$

where the Ts are the radial separation constants, and J_m is the Bessel function. The azimuthal eigenvalue m is an integer, as in the conical case. For the insulating boundary condition at the boundary of the cylinder $\rho = a$, we have in place of equations (12), (13), and (14), suppressing the subscript m (except in J_m):

$$D_T^2 \;=\; \frac{d^2}{dz^2} - T^2 \quad , \qquad (12')$$

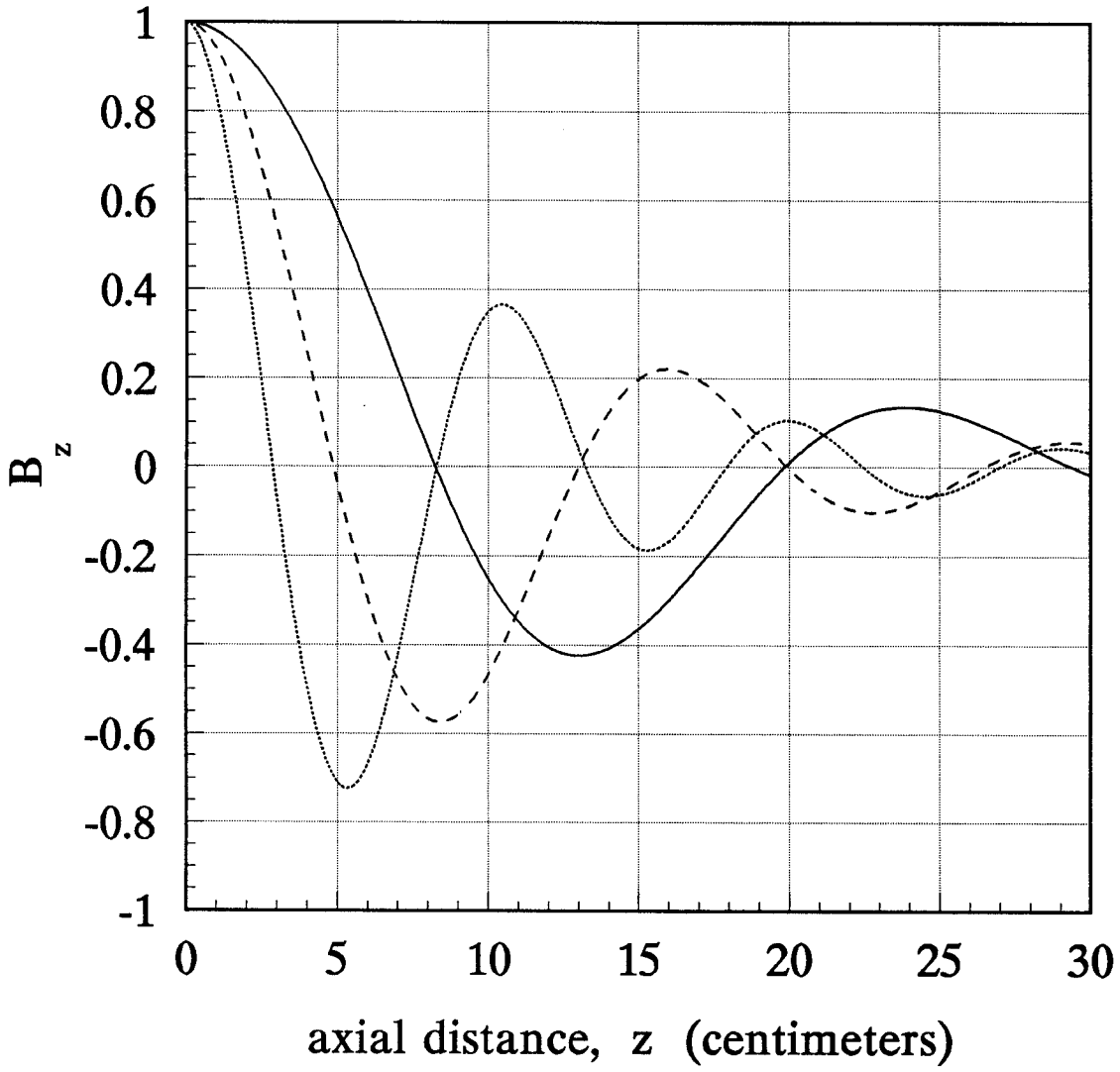

(a)

Figure 4: B_z on the axis of a parabola of revolution for $\sigma = 0.5$ (——), 1 (– – – –), and 2 ($\cdots$) $\mathrm{cm}^{-3}\ \mathrm{G}^{-1}$. **(a)** $a = 4\,\mathrm{cm}$, $b = 10\,\mathrm{cm}$; **(b)** $a = 2\,\mathrm{cm}$, $b = 5\,\mathrm{cm}$; **(c)** $a = 4\,\mathrm{cm}$, $b = 10\,\mathrm{cm}$; and **(d)** $a = 4\,\mathrm{cm}$, $b = 1000\,\mathrm{cm}$.

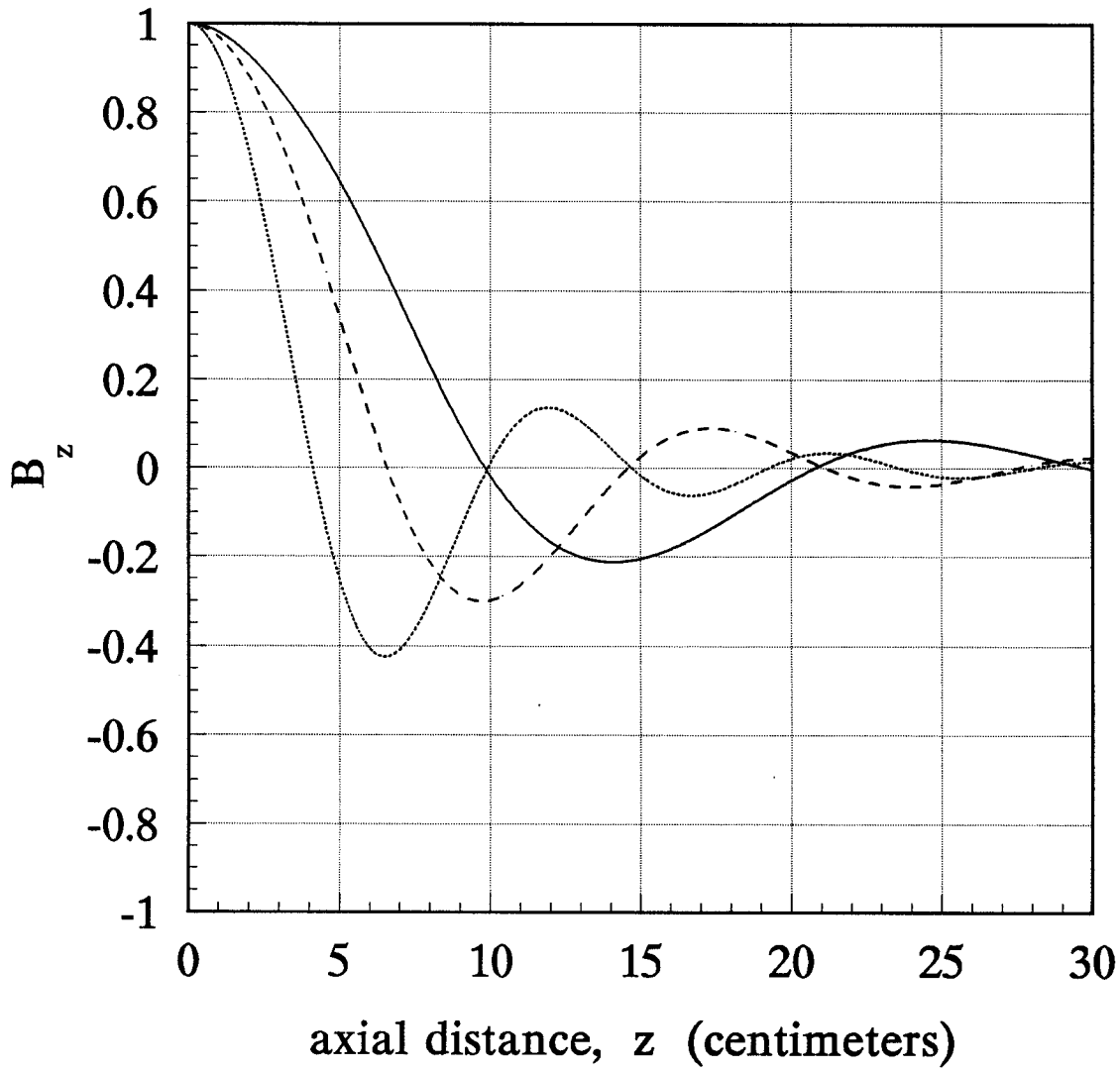
1
0.8
0.6
0.4
0.2
0
-0.2
-0.4
-0.6
-0.8
-1
B z
0
5
10
15
20
25
30
axial distance, z (centimeters)

(b)

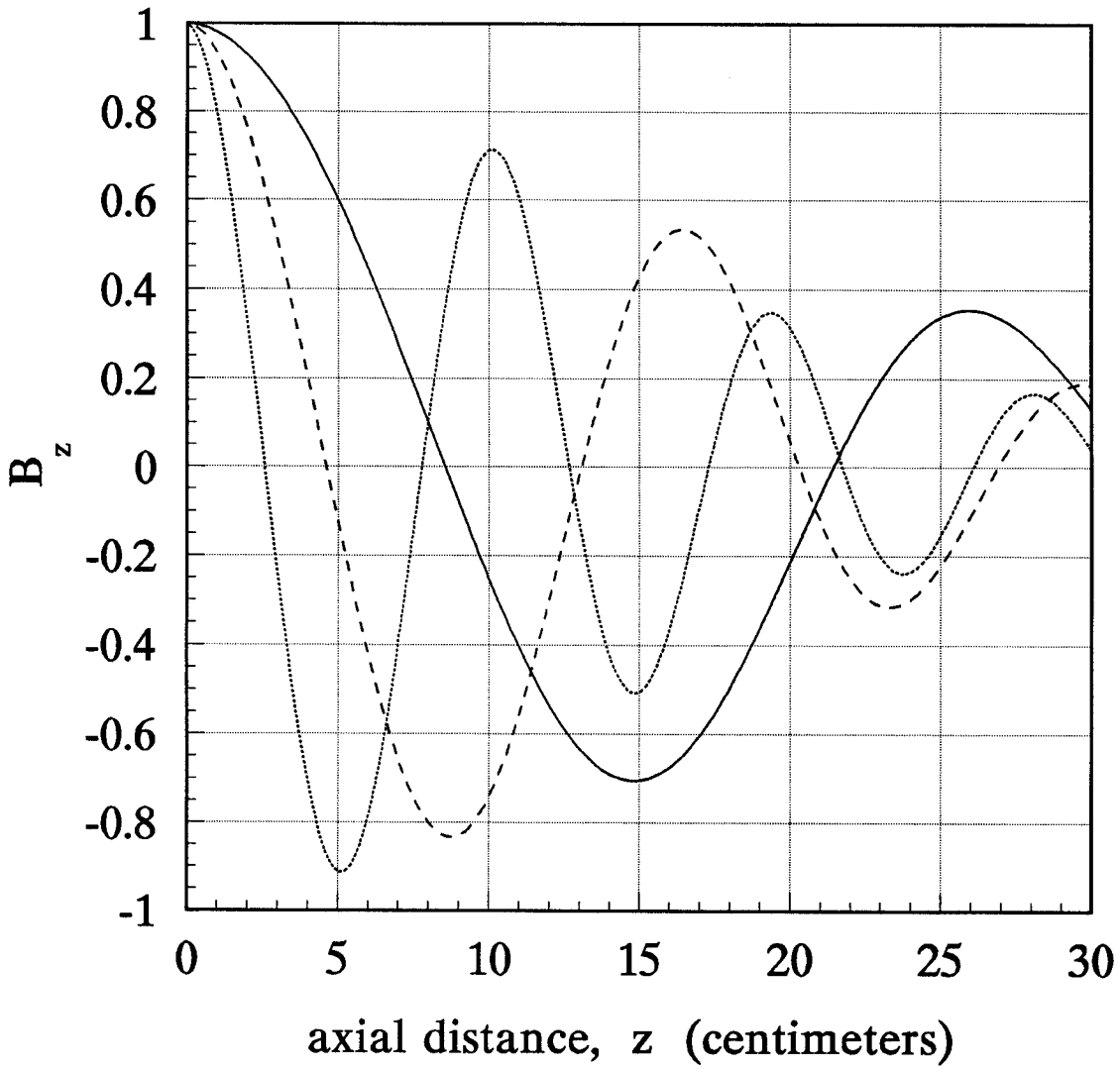
1
0.8
0.6
0.4
0.2
0
-0.2
-0.4
-0.6
-0.8
-1
B z
0
5
10
15
20
25
30
axial distance, z (centimeters)

(c)

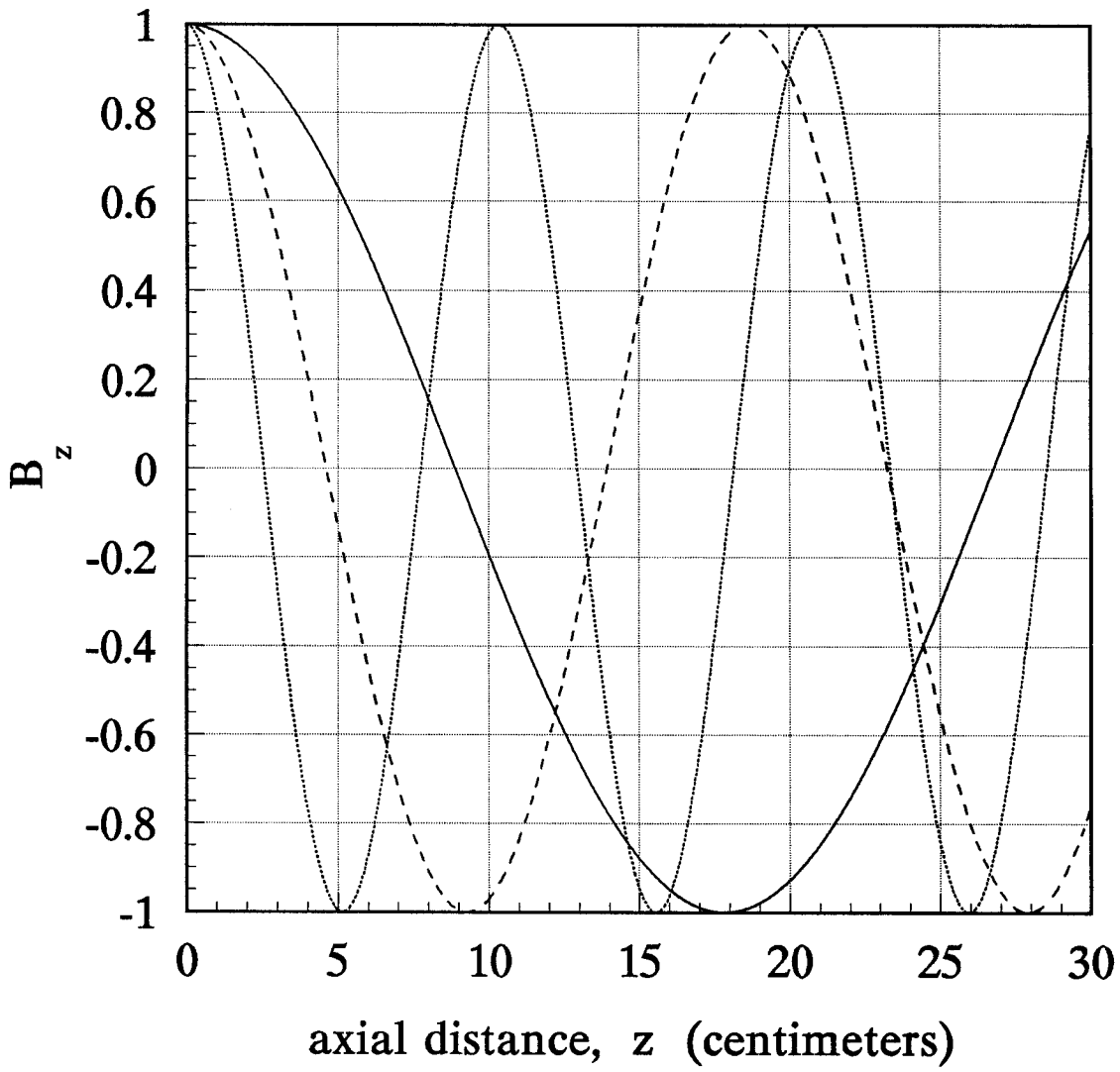
1
0.8
0.6
0.4
0.2
0
-0.2
-0.4
-0.6
-0.8
-1
B z
0
5
10
15
20
25
30
axial distance, z (centimeters)

(d)

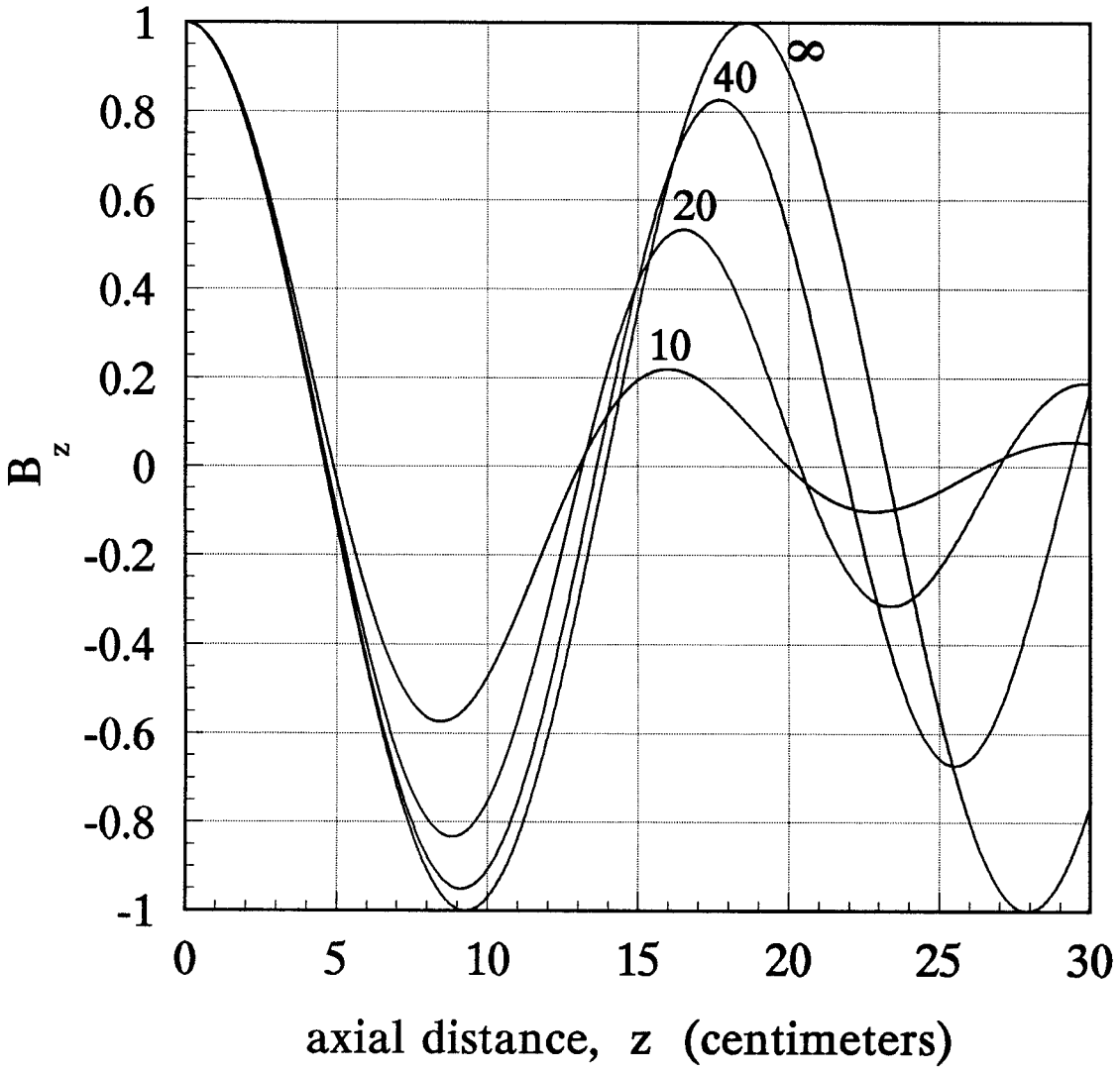

Figure 5: Same as Figure 4 for $a = 4\,\mathrm{cm}$, $b = 10,\ 20,\ 40$ and ∞ cm.

$$\sum_T \left\{ k_0^2 F_T - \beta_2 D_T^2 F_T - \beta_2' F_T' - \beta_3 T^2 F_T - \left(i\beta_1 D_T^2 G_T \right)' \right\} J_m \;=\; 0 \quad , \tag{13'a}$$

$$\sum_T \left\{ k_0^2 G_T - \beta_2 D_T^2 G_T + i\beta_1 F_T' \right\} J_m \;=\; 0 \quad , \tag{13'b}$$

$$\mu_0 J_r \;=\; \sum_T \left\{ \left[(1+\beta_2) J_m' \;-\; \frac{m}{\rho} \beta_1 J_m \right] F_T' \;+ \right.$$

$$\left. + \, i \left[\beta_1 J_m' - (1+\beta_2) \, \frac{m}{\rho} \, J_m \right] D_T^2 G_T \right\} \Big|_{\rho=a} \;=\; 0 \quad , \tag{14'}$$

where J_m' is the derivative of J_m with respect to ρ, and the primes of F and G denote derivatives with respect to z. If the βs are independent of z, F and G proportional to $\exp(ikz)$ satisfy equations (13′) and (14′) for each T in the summation and all z. Otherwise, as in the case of the cone, equation (14′) can only be satisfied for each T if $m = 0$. In the latter case, equation (15b) becomes

$$J_0'(Ta) \;= 0 \quad , \tag{15'b}$$

which yields a dispersion relation which is biquadratic in both T^2 and k^2:

$$k^2 \left(k^2 + T^2 \right) \beta_1^2 \;-\; \left[k_0^2 + \beta_2 \left(k^2 + T^2 \right) \right] \left[k_0^2 + \beta_2 \left(k^2 + T^2 \right) - \beta_3 T^2 \right] \;=\; 0,$$

which is a generalization of the familiar result of Chen (1992), $k^2 + T^2 = \alpha^2/k^2 = \left(k_0^2/\beta_1\right)^2 / k^2$, for $\beta_2 = \beta_3 = 0$. Combining equations (13′) and (14′) provides unique solutions for T^2 and k^2, which may in general be complex. In the case $m = 0$, where equation (15′ b) obtains, T is real, and for the parameter regime of equation (1), k^2 has a positive and a negative root corresponding to propagating and exponentiating solutions. In propagation through a flaring magnetic field, calculated for example by the methods of Section VI, the previously unidentified exponentiating solutions can play a small but crucial role in the self-consistent treatment of helicon waves.

References

Chen, F.F. (1994) "Helicon Plasma Sources" in *High Density Plasma Sources*, L. A. Popov, ed., Noyes.

Chen, F.F. (1992) *J. Vac. Sci. Technol. A* **10**, 1389-1401.

Morse, P.M. and Feshbach, H. (1953) *Methods of Theoretical Physics*, McGraw-Hill, New York, Toronto, London.

Peskoff, A. and Arnush, D. (1995) "Helicon Waves in a Flaring Magnetic Field, Part II: Solution in a Conical Region"

Solymar, L. (1959) *Inst. Elec. Engrs. – Proc.* **106**:B, supp. n13, pp. 121-128

Sporleder, F. and Unger, H.-G. (1979) "Waveguide tapers, transitions, and couplers", in *IEEE Electromagnetic Waves Series 6*, ed. Wait, J.R. et al. The Institute of Electrical and Electronic Engineers, London and New York.

Stix, T.H. (1992) *Waves in Plasmas*, American Institute of Physics, New York.

HELICON WAVES IN A FLARING MAGNETIC FIELD

Part II: Solution in a Conical Region

Arthur Peskoff and Donald Arnush

Biomathematics and Physiology Depts. and
Electrical Engineering Department

PPG-1539 March, 1995

Submitted to Plasma Physics and Controlled Fusion.

Helicon Waves in a Flaring Magnetic Field

Part II: Solution in a Conical Region

Arthur Peskoff* and **Donald Arnush**†

*Departments of Biomathematics and Physiology
UCLA School of Medicine
Los Angeles, CA 90095-1766

†Electrical Engineering Department
UCLA School of Engineering and Applied Science
Los Angeles, CA 90095-1594

Short Title: **Helicon Waves in a Flaring Magnetic Field**

Classification Numbers: 52.35.Hr

Abstract

It was found that the wave equation for a helicon wave in a cold plasma bounded transversely by a conical magnetic field is separable in spherical coordinates for $m = 0$, and the dependence on the radial coordinate (x) satisfies a fourth-order differential equation (Arnush and Peskoff 1995). A straight-forward numerical integration of the equation from x_1 to x_2 fails unless $x_2 - x_1$ is small, because of the existence of an exponentially growing solution to the equation. Consequently, a different approach is needed. Four independent solutions in the form of series in powers of x (PS) are obtained by expanding about $x = 0$. Each series is asymptotically proportional to e^x as $x \to \infty$. Four asymptotic expansions (AE) are obtained in the form of series in $1/x$ times $e^{\pm ix}$ and $e^{\pm x}$. The problem then is to extend the AEs backward to $x = 0$ by finding four linear combinations of the four PSs, each of which approaches one of the AEs in the limit $x \to \infty$ (i.e., only one of the four linear combinations approaches e^x). This is accomplished by first finding a double-integral representation of each PS, valid for all x, and then using its $x \to \infty$ limit to match each AE to a linear combination of the PSs. For special values of ℓ ($\ell = 4N - 1$ or $4N$, N an integer) the series in the AE terminates after a finite number of terms, and in such cases closed-form solutions (polynomials times exponentials) result that are exact representations of the solution for all x. Solutions are computed and illustrated for an outgoing wave using the closed-form solution for special values of ℓ and as a function of ℓ and x using the PS and AE, which have a large range of overlap.

I. Introduction

In the preceding paper (Arnush and Peskoff 1995, hereinafter referred to as I), a fourth-order differential equation was derived for describing a helicon wave in a conical region containing: (1) a magnetic field $\mathbf{B}_0$ with field lines directed radially outward from the origin of the spherical coordinate system centered at the apex of the cone, (2) a plasma with density proportional to $\mathbf{B}_0$, and (3) a conical boundary on which the normal component of current vanishes. An approximate, WKB-like solution for a propagating wave was obtained which is accurate except when close to the origin. This WKB-like solution was applied to a particular example of a flaring field where the boundary was a segment of a parabola of revolution. To consider more general cases in which behavior closer to the origin may be required, or in which reflected waves and higher mode generation may be important, it is necessary to find the complete solution to I, equation (17) (rewritten as equation (1) below.) This we do in the present paper.

In applications, it may be necessary to follow the solution over a large range of the nondimensional radial coordinate x. The direct numerical approach to solving an initial value problem by integrating the equation numerically, for example, using the Rünge-Kutta method (Dahlquist and Björck 1974) does not work in the present case for the following reason. There is a solution to the equation that grows exponentially with x. Consequently, any error in the initial value, or in the numerical computation, eventually will be amplified exponentially as x increases and will overshadow the desired solution. Our attempts to solve the equation numerically on a PC in double precision (16 digits) failed for radial distances $(x_2 - x_1) \gtrsim 20$, and so a different approach is taken.

Instead of direct numerical integration, we find analytic functions which represent the solutions to the equation. The usual special functions that arise in mathematical physics (e.g., Bessel, Legendre and hypergeometric functions) are solutions to second-order differential equations. For the present fourth-order equation, no such previously obtained solutions are available.

In Section II, we find four convergent series solutions by expanding about $x = 0$ using the method of Frobenius (Morse and Feshbach 1953). Each of these four series is asymptotically proportional to e^x for large x. However, for large x, equation (1) has four independent solutions that approach $e^{\pm ix}$ and $e^{\pm x}$. For physical problems of interest we want incoming and outgoing wave solutions ($e^{\pm ix}$) which extend back to $x = 0$. Consequently we must remove the exponentially growing components from the Frobenius solutions. This is done

by finding four linear combinations of the four series solutions which approach $e^{\pm ix}$ and $e^{\pm x}$, respectively, as $x \to \infty$. In Section III, we obtain four asymptotic expansions for the solutions to I, equation (17), in the form of series in inverse powers of the normalized radial distance x (see I, preceding equation (17) for the definition of x) times $e^{\pm ix}$ or $e^{\pm x}$. The range of validity in x is similar to the WKB-like solution in I. However, for particular integer values of the eigenvalue ℓ ($\ell = 4N,\ 4N-1;\quad N = 0, 1, 2, \ldots$), the series terminates after $\ell - 2$ terms and the asymptotic result becomes exact for all x. In Section IV, a double-integral representation of the solution is obtained. In Section V, by asymptotic evaluation of the integral representation in the limit of large x, the connection between the series expansion about $x = 0$ and the large-x asymptotic expansions is made. The general solution is computed using the appropriate linear combination of the series solutions for small x and the asymptotic expansion for large x. Results of the computation are shown for an outgoing wave.

II. Power Series Expansion

To develop the power series representation of the solution to I equation (17), i.e.

$$\frac{d^4}{dx^4} H_\ell - \frac{\ell(\ell+1)}{x^2} \frac{d^2}{dx^2} H_\ell - H_\ell = 0 \quad , \tag{1}$$

we assume that

$$H(x) = \sum_{n=0}^{\infty} A_n x^{n+s} \quad , \tag{2}$$

and insert equation (2) in equation (1). For compactness, we have omitted the ℓ subscript on $H_\ell(x)$. It is assumed in equation (2) and henceforth that $H(x)$, A_n, and s depend on ℓ, without so indicating. The requirement that $A_0 \neq 0$ provides four possible values for s:

$$(s_1,\ s_2,\ s_3,\ s_4) = (\ell+3, 1, 0, 2-\ell) \quad . \tag{3}$$

Gathering the coefficients of equal powers of x and requiring that they vanish provides the recursion relation

$$(n+s-s_1)(n+s-s_2)(n+s-s_3)(n+s-s_4) A_n = A_{n-4} \quad . \tag{4}$$

Setting $A_0 = 1$, we may solve for A_n provided ℓ does not take on the particular values

$$\ell = 4N+2,\ 4N+3, \text{ or } 2N-\tfrac{1}{2} \quad , \tag{5}$$

where N is a positive integer. With that restriction, we obtain the four independent solutions:

$$H(s_j, x) = x^{s_j} \sum_{n=0}^{\infty} \prod_{\substack{i=1 \\ i \neq j}}^{4} \frac{\Gamma\left(1 + (s_j - s_i)/4\right)}{\Gamma\left(n + 1 + (s_j - s_i)/4\right)} \frac{1}{n!} \left(\frac{x}{4}\right)^{4n} \quad . \tag{6}$$

Morse and Feshbach (1953) provide a straightforward but lengthy algorithm for calculating H when ℓ takes on the values forbidden by equation (5). We will not repeat it here because, since ℓ is a continuous variable and H is a continuous function for a given ℓ, those values are easily avoided in any practical calculation, and their inclusion makes no significant difference in the calculated value of the function. The series equation (6) converges in the finite x-plane. For large x, the large n successive terms of each series approach every fourth term in the series for e^x. Consequently, it can be shown by comparison that all four series grow exponentially.

III. Asymptotic Expansion

In the $x \to \infty$ limit, equation (1) approaches the simpler fourth-order equation

$$\frac{d^4 H}{dx^4} - H = 0 \quad . \tag{7}$$

Four independent solutions to this equation are

$$H(x) = e^{px} \quad , \tag{8}$$

where $p = \pm i, \pm 1$ is one of the four roots of $p^4 = 1$. The four roots correspond to an outgoing wave, an incoming wave, exponential growth, and exponential decay, respectively.

To develop an asymptotic expansion for the solution to equation (1), first we assume a form for the growing exponential solution, as $x \to \infty$,

$$H(x) = e^x w(x) \sim e^x \sum_{n=0}^{M} B_n \frac{1}{x^n} \quad , \tag{9}$$

where $(M + 1)$ is an optimum number of terms used to represent $H(x)$.

Substituting equation (9) in the differential equation (1) for $H(x)$ yields the differential equation for $w(x)$,

$$\frac{d^4 w}{dx^4} + 4 \frac{d^3 w}{dx^3} + \left(6 - \frac{\ell(\ell+1)}{x^2}\right) \frac{d^2 w}{dx^2} + \left(4 - \frac{2\ell(\ell+1)}{x^2}\right) \frac{dw}{dx} - \frac{\ell(\ell+1)}{x^2} w = 0 \quad . \tag{10}$$

Substituting the series in inverse powers of x from equation (9) in equation (10), and equating terms with like powers of x, we get the recursion relation

$$
\begin{aligned}
&B_0 = 1, \qquad B_1 = -\frac{\ell(\ell+1)}{4} \quad , \qquad B_2 = -\frac{\ell(\ell+1)}{32}\Big[12 - \ell(\ell+1)\Big] \quad , \\
&4nB_n = \quad \Big[6n(n-1) - \ell(\ell+1)\Big] B_{n-1} - 2(n-2)\Big[2n(n-1) - \ell(\ell+1)\Big] B_{n-2} \\
&\qquad\qquad -(n-2)(n-3)\Big[n(n-1) - \ell(\ell+1)\Big] B_{n-3} \qquad \text{for} \quad n > 2 \quad .
\end{aligned}
\tag{11}
$$

By computing the B_n for integer values of ℓ using recursion relation (11), we find that if $\ell = 4N-1$ or $4N$ where $N = 1, 2, 3, \ldots$, then $B_n = 0$ for $n \geq \ell - 1$. Consequently, for these particular values of ℓ, the series in equation (11) terminates after a finite number of terms. For these values of ℓ, it yields an exact solution of equation (1) in the form of a polynomial in $1/x$ times an exponential. This solution is valid for all x. For other values of ℓ, the series does not terminate, and the expansion is only asymptotic to the solution. In the computations described below, we find that truncating the asymptotic series after the B_n term, where n is the largest integer less than ℓ, yields an accurate representation of the solution for large x, i.e., $x \gg \ell$.

If p is one of the four roots of $p^4 = 1$, and if $H(x)$ is a solution of equation (1), then $H(px)$ is also a solution. Consequently, four independent asymptotic solutions of equation (1) are given by $H(px)$. We denote these four solutions by $h_{\ell,1}(x)$, $h_{\ell,2}(x)$, $h_{\ell,3}(x)$, and $h_{\ell,4}(x)$. As an example, for $\ell = 3$,

$$
\begin{aligned}
h_{3,1}(x) &= \left(1 + \frac{3i}{x}\right) e^{ix} \\
h_{3,2}(x) &= \left(1 - \frac{3i}{x}\right) e^{-ix} \\
h_{3,3}(x) &= \left(1 - \frac{3}{x}\right) e^{x} \\
h_{3,4}(x) &= \left(1 + \frac{3}{x}\right) e^{-x} \quad ;
\end{aligned}
\tag{12a}
$$

and for $\ell = 4$,

$$
\begin{aligned}
h_{4,1}(x) &= \left(1 + \frac{5i}{x} - \frac{5}{x^2}\right) e^{ix} \\
h_{4,2}(x) &= \left(1 - \frac{5i}{x} - \frac{5}{x^2}\right) e^{-ix}
\end{aligned}
$$

$$h_{4,3}(x) = \left(1 - \frac{5}{x} + \frac{5}{x^2}\right) e^{x}$$

$$h_{4,4}(x) = \left(1 + \frac{5}{x} + \frac{5}{x^2}\right) e^{-x} \quad . \tag{12b}$$

Figure 1 shows the real and imaginary parts of the outgoing waves, $h_{3,1}$, $h_{4,1}$, $h_{7,1}$, and $h_{8,1}$.

Equations (12a) and (12b) indicate that all of the eight solutions diverge at $x = 0$. One can construct an outgoing wave solution that does not become infinite at the origin, using the solutions in (12a) and (12b), by taking the linear combinations

$$h_{3,5}(x) = h_{3,1} - i\, h_{3,4}$$

$$h_{4,5}(x) = h_{4,1} + h_{4,4} \quad . \tag{12c}$$

These are two outgoing waves for $\ell = 3$ and $\ell = 4$ that are finite at the origin. In fact, we will show later that these are just two special cases of the general result that

$$h_{\ell,5} = h_{\ell,1} + e^{i\pi\,\ell/2}\, h_{\ell,4} \tag{12d}$$

is an outgoing wave, finite everywhere. In the large-x asymptotic limit, $h_{\ell,4}$ is exponentially small, and consequently $h_{\ell,1}$ and $h_{\ell,5}$ have the same asymptotic limit.

In figure 1, the real and imaginary parts of $h_{\ell,5}$ for $\ell = 3, 4, 7$ and 8 are shown, along with the corresponding $h_{\ell,1}$. Note that Re $\{h_{\ell,1}\}$ for $\ell = 3$ and 7, and $Im\,\{h_{\ell,1}\}$ for $\ell = 4$ and 8 are not infinite at $x = 0$. This may be verified by multiplying the polynomials in equations (12a) and (12b) by the series expansions of the exponentials, and substituting in equation (12c).

Each of the convergent series solutions in equation (6) can be decomposed into a linear combination of four functions, each of which approaches one of the four asymptotic solutions e^{px} in the $x \to \infty$ limit. Similarly, each of these four functions can be expressed as a linear combination of the four convergent series. If, for example, we wish to calculate the field of a wave that is outgoing in the $x \to \infty$ limit, we need to find this linear combination in order to continue the asymptotic solution backward to $x = 0$. To do this, first we need to obtain the asymptotic behavior of the four convergent series of equation (9) for large x. In the next two sections, the linear combinations will be calculated by first finding a double-integral representation of $H_\ell(x)$, and then finding its asymptotic limit.

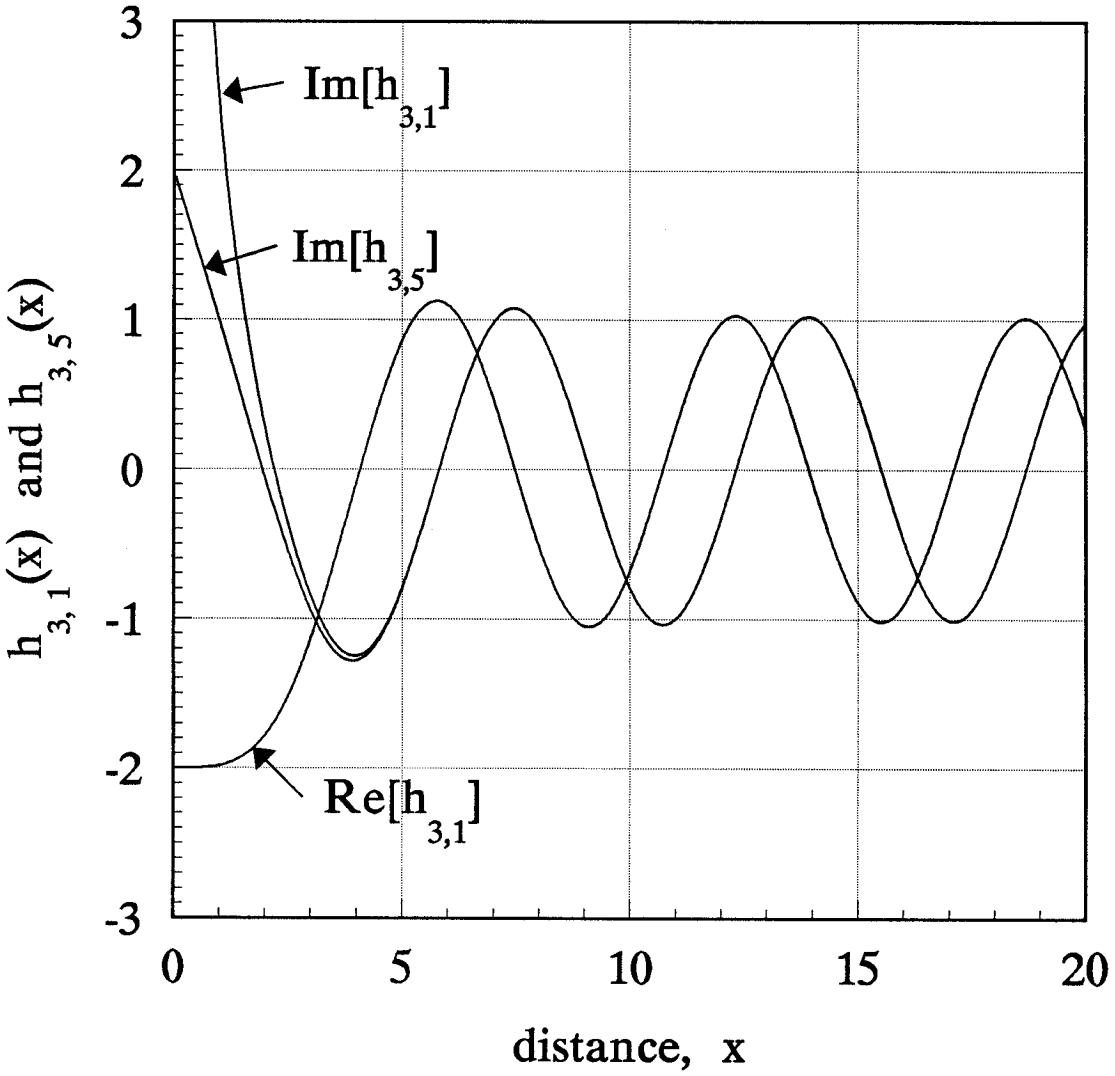

(a)

Figure 1: Exact solutions for the real and imaginary parts of the "pure" outgoing wave, $h_{\ell,1}(x)$, for $\ell = 3$, 4, 7 and 8. The exact solutions for the imaginary part of the outgoing wave finite at the origin $\mathrm{Im}\,[\,h_{\ell,5}(x)\,]$, is shown for $\ell = 3$ and 7, and $\mathrm{Re}\,[\,h_{\ell,5}(x)\,]$ is shown for $\ell = 4$ and 8. For $\ell = 3$ and 7, $\mathrm{Re}\,[\,h_{\ell,5}(x)\,] = \mathrm{Re}\,[h_{\ell,1}(x)\,]$. For $\ell = 4$ and 8, $\mathrm{Im}\,[h_{\ell,5}(x)] = \mathrm{Im}\,[h_{\ell,1}(x)\,]$.

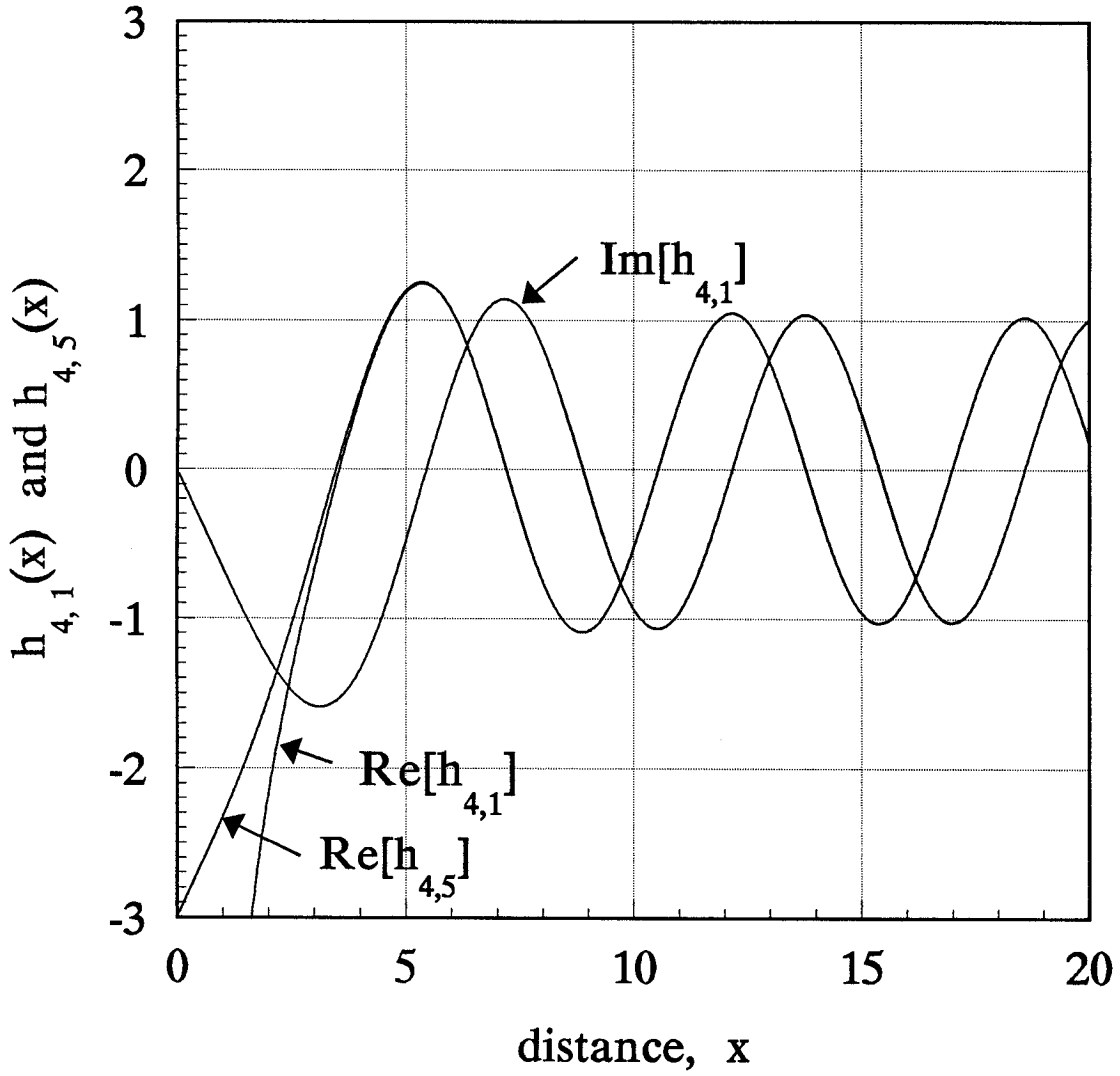
3
2
1
0
-1
-2
-3
0
5
10
15
20
h 4, 1 (x) and h 4, 5 (x)
distance, x
Im[h 4,1]
Re[h 4,1]
Re[h 4,5]

(b)

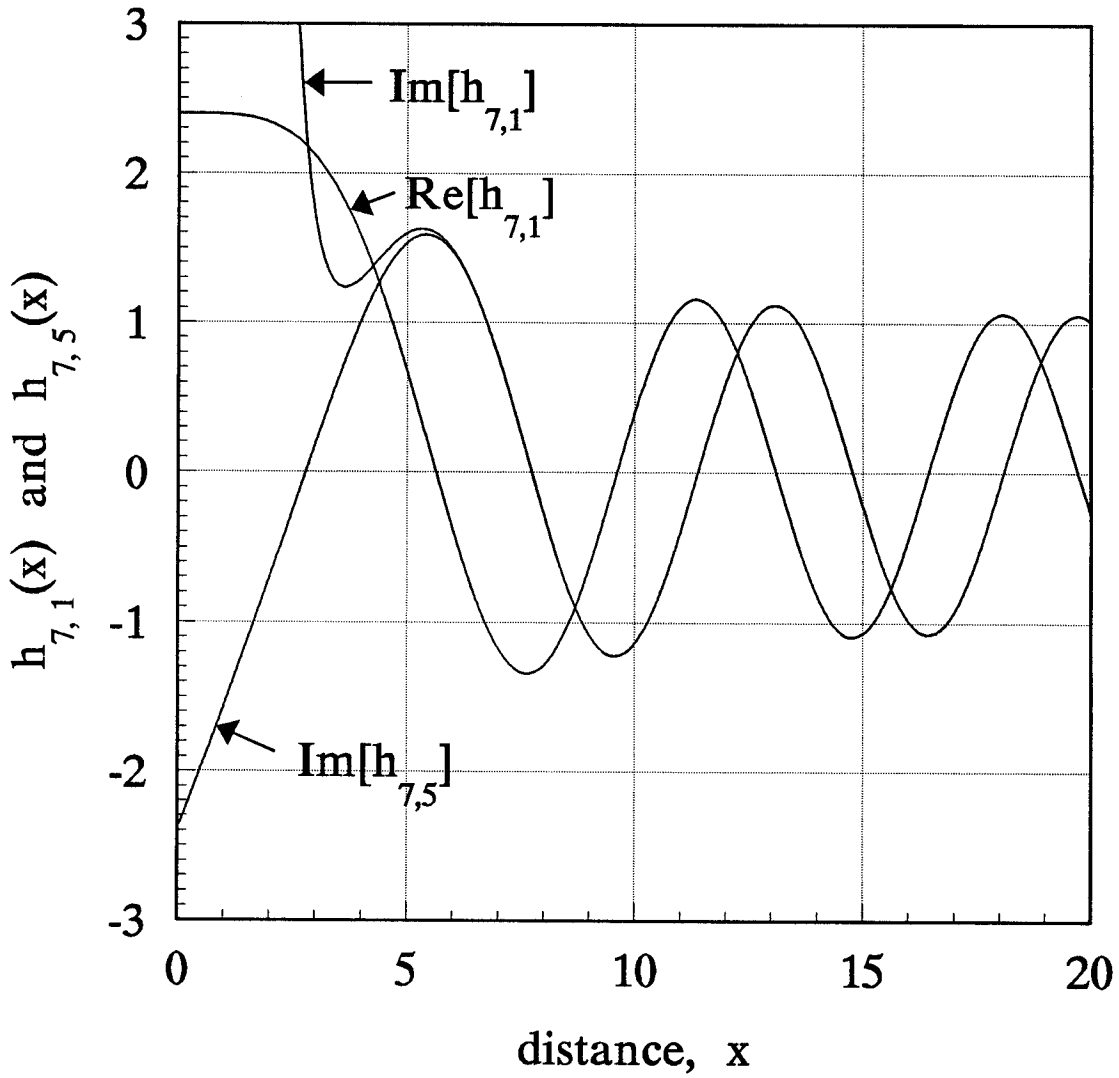
3
2
1
0
-1
-2
-3
0
5
10
15
20
Im[h7,1]
Re[h7,1]
Im[h7,5]
h7,1(x) and h7,5(x)
distance, x

(c)

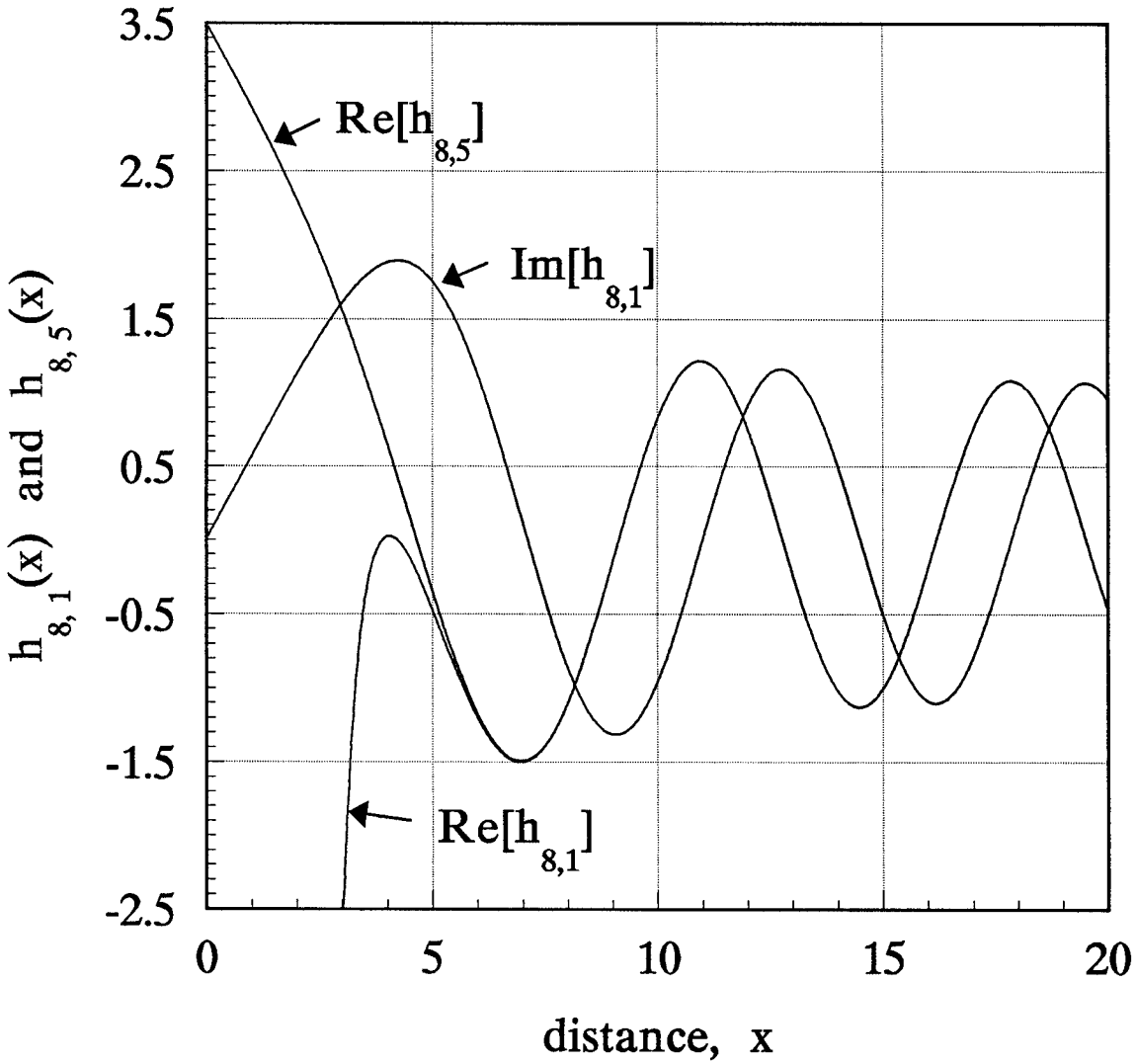
3.5
2.5
1.5
0.5
-0.5
-1.5
-2.5
0
5
10
15
20
Re[h8,5]
Im[h8,1]
Re[h8,1]
h8,1(x) and h8,5(x)
distance, x

(d)

IV. Integral Representation of $\mathbf{H_\ell(x)}$

We start with the two series for the ordinary and modified Bessel functions of order ℓ (Abramowitz and Stegun 1964), and define a new function, $\Phi(\ell, z)$, by

$$\Phi(\ell, z) = \tfrac{1}{2}\,(z/2)^{-\ell}\,[J_\ell(z) + I_\ell(z)]$$

$$= \sum_{n=0}^{\infty} \frac{(z/2)^{4n}}{(2n)!\,\Gamma(2n+\ell+1)} \quad , \tag{13}$$

where the $(z/2)^{2n}$ terms in the J_ℓ and I_ℓ series with n odd have canceled. We will use two integral transforms of $\Phi(\ell, z)$ that will transform the sum in equation (13) into the sum in equation (6).

First, we use a known integral representation of the Beta function (Abramowitz and Stegun 1964):

$$\int_0^1 t^{p-1/2}(1-t)^{q-1/2}dt = B\left(p+\tfrac{1}{2}\ ,\ q+\tfrac{1}{2}\right) = \frac{\Gamma\left(p+\frac{1}{2}\right)\Gamma\left(q+\frac{1}{2}\right)}{\Gamma(p+q+1)} \quad ,$$

which is valid for $p > -\frac{1}{2}$, $q > -\frac{1}{2}$, and the duplication formula for the gamma function,

$$\Gamma(2p) = \pi^{-1/2}\,2^{2p-1}\,\Gamma(p)\,\Gamma\left(p+\tfrac{1}{2}\right) \quad ,$$

to obtain

$$\int_0^1 t^{p-1/2}\,(1-t)^{q-1/2}\,dt = \pi^{1/2}\,2^{-2p}\,\frac{\Gamma(2p+1)\,\Gamma\left(q+\frac{1}{2}\right)}{\Gamma(p+1)\,\Gamma(p+q+1)} \quad . \tag{14}$$

Next, we define an integral transform of $\Phi(\ell, z)$ by

$$\Psi(a,\,b,\,y) = \int_0^1 \Phi\left(2a,\,yt^{1/4}\right)\,(1-t)^{b-1/2}\,t^{-1/2}\,dt$$

$$= \sum_{n=0}^{\infty} \frac{(y/2)^{4n}\int_0^1 t^{n-1/2}\,(1-t)^{b-1/2}\,dt}{(2n)!\,\Gamma(2n+2a+1)}$$

$$= \pi^{1/2}\,\Gamma\left(b+\tfrac{1}{2}\right) \sum_{n=0}^{\infty} \frac{(y^2/8)^{2n}}{n!\,\Gamma(2n+2a+1)\,\Gamma(n+b+1)} \tag{15}$$

for $b > -\frac{1}{2}$. The last equality in equation (15) was obtained using equation (14), with $p = n$ and $q = b$ to evaluate the integral. In equation (15) we have eliminated the unwanted $(2n)!$ that was present in the denominator of equation (13), and introduced the $n!$ and $\Gamma(n+b+1)$ needed in the denominator of equation (6).

Finally, we define an integral transform of $\Psi(a,b,y)$ by

$$\Omega(a,b,c,x) = \int_0^1 \Psi\left(a,b,xs^{1/4}\right)(1-s)^{c-a-1/2}\,s^{a-1/2}\,ds$$

$$= \pi^{1/2}\,\Gamma\left(b+\tfrac{1}{2}\right)\sum_{n=0}^{\infty}\frac{(x^2/8)^{2n}\int_0^1 s^{n+a-1/2}(1-s)^{c-a-1/2}\,ds}{n!\,\Gamma(2n+2a+1)\,\Gamma(n+b+1)}$$

$$= 2^{-2a}\,\pi\,\Gamma\left(b+\tfrac{1}{2}\right)\Gamma\left(c-a+\tfrac{1}{2}\right)\sum_{n=0}^{\infty}\frac{(x/4)^{4n}}{n!\,\Gamma(n+a+1)\,\Gamma(n+b+1)\,\Gamma(n+c+1)} \qquad (16)$$

for $a > -\frac{1}{2}$, $b > -\frac{1}{2}$, $c-a > -\frac{1}{2}$. The last equality in equation (16) was obtained using equation (14), with $p = n+a$ and $q = c-a$. In equation (16) we have eliminated the $\Gamma(2n+2a+1)$ that was present in the denominator of equation (15), and obtained the final two gamma functions, $\Gamma(n+a+1)$ and $\Gamma(n+c+1)$, needed in the denominator of equation (6).

For convenience, we define $\tilde{H}$, which is the sum in equation (6) without the factors that are independent of n:

$$\tilde{H}(a,b,c,x) = \sum_{n=0}^{\infty}\frac{(x/4)^{4n}}{n!\,\Gamma(n+a+1)\,\Gamma(n+b+1)\,\Gamma(n+c+1)} \qquad (17)$$

Combining equations (15) and (16), we have the double-integral representation for $\tilde{H}$,

$$\tilde{H}(a,b,c,x) = \frac{(x/4)^{-2a}}{2\pi\,\Gamma\left(b+\frac{1}{2}\right)\Gamma\left(c-a+\frac{1}{2}\right)}\int_0^1 s^{a/2-1/2}(1-s)^{c-a-1/2}$$

$$\left(\int_0^1 t^{-a/2-1/2}(1-t)^{b-1/2}\left[J_{2a}\left(xs^{1/4}t^{1/4}\right)+I_{2a}\left(xs^{1/4}t^{1/4}\right)\right]dt\right)ds \qquad (18)$$

for $a > -\frac{1}{2}$, $b > -\frac{1}{2}$, $c-a > -\frac{1}{2}$.

V. Asymptotic Behavior of Equation (6) for $|\,x\,| \longrightarrow \infty$

Using the integral representation of equation (18) and the known large-argument asymptotic behavior of the Bessel functions (Abramowitz and Stegun 1964),

$$J_{2a}\left(xs^{1/4}t^{1/4}\right) \sim (\pi x/2)^{-1/2}\,s^{-1/8}\,t^{-1/8}\cos\left(xs^{1/4}t^{1/4}-\left(a+\tfrac{1}{4}\right)\pi\right)$$

$$I_{2a}\left(xs^{1/4}t^{1/4}\right) \sim (2\pi x)^{-1/2}\,s^{-1/8}\,t^{-1/8}\exp\left(xs^{1/4}t^{1/4}\right) \quad ,$$

for real arguments of J_{2a} and I_{2a}, we can evaluate the asymptotic behavior of equation (18) in the $x \to \infty$ limit. The contribution to the integral from the I_{2a} term grows exponentially, whereas the contribution from J_{2a} decreases with increasing x because of the rapid oscillation of J_{2a}. Consequently, J_{2a} will not contribute to the leading term in the asymptotic expansion and can be ignored. We have, therefore,

$$\tilde{H}(a,b,c,x) \sim \frac{(2\pi)^{-3/2}\, x^{-1/2}\, (x/4)^{-2a}}{\Gamma\left(b+\frac{1}{2}\right)\,\Gamma\left(c-a+\frac{1}{2}\right)} \int_0^1 s^{a/2-1/2}(1-s)^{c-a-1/2} \left(\int_0^1 t^{-a/2-1/2}(1-t)^{b-1/2}\, s^{-1/8}\, t^{-1/8} \exp\left(x s^{1/4} t^{1/4}\right) dt\right) ds \quad . \tag{19}$$

Furthermore, in the $x \to \infty$ limit, the major contribution to the double integral in equation (18) or (19) comes from the immediate vicinity of $s = 1$, $t = 1$. To obtain the leading term in the asymptotic expansion, we can replace $s^{a/2-5/8}$ and $t^{-a/2-5/8}$ by 1. (To find higher order terms, we could expand about $s = 1$ and $t = 1$, but for our purposes we only need this first term.)

Making a change of variables, $s = u^4$, $t = v^4$, we can make the additional simplifications,

$$\begin{aligned} (1-s)^{c-a-1/2} &\to \left[4(1-u)\right]^{c-a-1/2} \quad \text{as} \quad u \to 1 \\ (1-t)^{b-1/2} &\to \left[4(1-v)\right]^{b-1/2} \quad \text{as} \quad v \to 1 \quad . \end{aligned}$$

Introducing these change of variables and limiting forms in equation (19), we have

$$\tilde{H}(a,b,c,x) \sim \frac{\pi^{-3/2}\, 2^{2a+2b+2c+1/2}\, x^{-2a-1/2}}{\Gamma\left(b+\frac{1}{2}\right)\,\Gamma\left(c-a+\frac{1}{2}\right)} \cdot \int_0^1 (1-u)^{c-a-1/2} \left(\int_0^1 (1-v)^{b-1/2}\, e^{xuv}\, dv\right) du \quad . \tag{20}$$

To obtain the asymptotic limit of equation (20), we first evaluate the asymptotic limit of the following integral in the $\beta \to \infty$ limit:

$$\int_0^1 (1-\xi)^\alpha\, e^{\beta\xi}\, d\xi \;=\; \beta^{-\alpha-1}\, e^\beta \int_0^\beta w^\alpha\, e^{-w}\, dw \;\to\; \beta^{-\alpha-1}\, e^\beta\, \Gamma(\alpha+1) \quad , \tag{21}$$

where $1-\xi = w/\beta$, and the integral representation of the gamma function is used to obtain the limit. Using equation (21) twice in succession in equation (20), as $x \to \infty$,

$$\int_0^1 (1-u)^{c-a-1/2} \left(\int_0^1 (1-v)^{b-1/2}\, e^{xuv}\, dv\right) du \to \Gamma\left(b+\tfrac{1}{2}\right) x^{-b-1/2} \int_0^1 (1-u)^{c-a-1/2}\, e^{xu}\, du$$

$$\rightarrow \quad \Gamma\left(b+\tfrac{1}{2}\right)\Gamma\left(c-a+\tfrac{1}{2}\right)x^{a-b-c-1}\,e^{x} \quad . \tag{22}$$

Substituting equation (22) in equation (20),

$$\tilde{H}(a,b,c,x) \;\sim\; \pi^{-3/2}\,2^{2a+2b+2c+1/2}\,x^{-a-b-c-3/2}\,e^{x} \quad . \tag{23}$$

In the derivation of equation (18), it was required that $a > -\frac{1}{2}$, $b > -\frac{1}{2}$, and $c-a > -\frac{1}{2}$. By making the correspondence between a, b, and c in equation (17), and $s_j - s_k$ in equations (3) and (6), we find that the inequalities can be satisfied for $j = 1,2$, and 3. But for the $s_j = s_4 = 2-\ell$ with $\ell > \frac{1}{2}$, no selection of a, b, and c satisfies the inequalities, the integral representation for H diverges, and the derivation of equation (18) in this case is not valid. However, by analytic continuation (Morse and Feshbach 1953) the asymptotic result of equations (22) and (23) must be valid, even in this case. This must be true because equation (20) is an analytic function of a, b, or c, which we have shown agrees over a range of a, b, or c with the leading term in the asymptotic expansion of $H_\ell(x)$, but is itself analytic over all a, b, c.

Inserting the factors in equation (6) that were omitted from equation (17), and using the result

$$a+b+c \;=\; s-\tfrac{3}{2} \quad ,$$

obtained from equation (3), we have the asymptotic result as $x \rightarrow \infty$:

$$\begin{aligned} H(s,x) &= C_s\,e^{x} \\ C_s &= (2\pi)^{-3/2}\,2^{2s-1}\,\Gamma\left(1+\frac{s-\ell-3}{4}\right)\Gamma\left(1+\frac{s-1}{4}\right)\Gamma\left(1+\frac{s}{4}\right)\Gamma\left(1+\frac{s+\ell-2}{4}\right) \end{aligned} \tag{24}$$

VI. Connecting the x = 0 and x = ∞ Expansions

We now can find the four linear combinations of the four solutions to equation (6) around $x = 0$ that approach e^{ix} (outgoing wave), e^{-ix} (incoming wave), e^{x} (growing exponential), and e^{-x} (decaying exponential) as $x \rightarrow +\infty$. By exploiting the symmetry properties of $H(s_j,x)$ in equation (6), we may generalize the result of the previous section to deduce the asymptotic behavior as $x \rightarrow -\infty$, and $\pm i\infty$ from the behavior as $x \rightarrow +\infty$. Equation (6) may be written as

$$H(s,x) \;=\; x^{s}\,F_s\left(x^4\right) \quad . \tag{25}$$

Since F_s is a function of x^4, we see that

$$\lim_{x\to\infty} F_s\left(x^4\right) \;=\; \lim_{x\to-\infty} F_s\left(x^4\right) \;=\; \lim_{x\to\pm i\infty} F_s\left(x^4\right) \;=\; |\,x\,|^{-s}\, C_s\, e^{|x|} \quad , \tag{26}$$

where C_s is given by equation (24). Substituting equation (26) in equation (25),

$$\begin{aligned} \lim_{x\to-\infty} H(s,x) \;&=\; \lim_{x\to-\infty} x^s\,|\,x\,|^{-s}\, C_s\, e^{|x|} \;=\; e^{i\pi s}\, C_s\, e^{|x|} \\ \lim_{x\to\pm i\infty} H(s,x) \;&=\; \lim_{x\to\pm i\infty} x^s\,|\,x\,|^{-s}\, C_s\, e^{|x|} \;=\; e^{\pm i\pi s/2}\, C_s\, e^{|x|} \end{aligned} \quad , \tag{27}$$

in which we have defined the phase of x in the range $-\pi < (phase\ of\ x) \leq \pi$. Using the results in equation (27), we can write down the linear combination of the four asymptotic solutions for $|\,x\,| \to \infty$ that give the asymptotically correct $H(s,x)$ along the positive and negative real and imaginary axes:

$$\lim_{|x|\to\infty} H(s,x) \;=\; C_s\left[e^{-i\pi s/2}\, e^{ix} \;+\; e^{i\pi s/2}\, e^{-ix} \;+\; e^{x} \;+\; e^{i\pi s}\, e^{-x}\right] \quad . \tag{28}$$

Denoting the analytic continuation of the four $|\,x\,| \to \infty$ solutions $e^{\pm ix}$ and $e^{\pm x}$ in equation (28) by $h_{\ell,1}(x)$, $h_{\ell,2}(x)$, $h_{\ell,3}(x)$, and $h_{\ell,4}(x)$, respectively, and deleting the subscript ℓ for convenience, it follows that

$$H(s,x) \;=\; C_s\left[e^{-i\pi s/2}\, h_1(x) \;+\; e^{i\pi s/2}\, h_2(x) \;+\; h_3(x) \;+\; e^{i\pi s}\, h_4(x)\right] \quad , \tag{29}$$

where, again, s can take on the four values, $s_1 = \ell + 3$, $s_2 = 1$, $s_3 = 0$, and $s_4 = 2 - \ell$. Equation (29) is a system of four equations that can be inverted to obtain h_1, h_2, h_3, and h_4, which are each a linear combination of the four functions $H\,(s_j, x)$, $j = 1, 2, 3, 4$, and which approach e^{ix}, e^{-ix}, e^{x}, and e^{-x}, respectively, as $x \to \infty$.

Writing equation (29) in matrix form, we have

$$\begin{bmatrix} H(\ell+3,\,x)\,/\,C_{\ell+3} \\ H(1,x)\,/\,C_1 \\ H(0,x)\,/\,C_0 \\ H(2-\ell,\,x)\,/\,C_{2-\ell} \end{bmatrix} = \begin{bmatrix} i\,e^{-i\pi\ell/2} & -ie^{i\pi\ell/2} & 1 & -e^{i\pi\ell} \\ -i & i & 1 & -1 \\ 1 & 1 & 1 & 1 \\ -e^{i\pi\ell/2} & -e^{-i\pi\ell/2} & 1 & e^{-i\pi\ell} \end{bmatrix} \begin{bmatrix} h_1(x) \\ h_2(x) \\ h_3(x) \\ h_4(x) \end{bmatrix} \tag{30}$$

This matrix may be inverted and, after lengthy algebra, the result is

$$h_i(x) \;=\; \frac{1}{D} \sum_{j=1}^{4} A_{ij}\, H\,(s_j,\,x)\;/\,C_{s_j} \quad , \tag{31}$$

where

$$D = 8\left(\cos\pi\ell + \sin^3\frac{\pi\ell}{2} + \cos^3\frac{\pi\ell}{2}\right) \quad , \tag{32}$$

and

$$\left[A_{ij}\right] = \begin{bmatrix} A & iB & B & iA^* \\ A^* & -iB^* & B^* & -iA \\ C & B & B & C^* \\ E & -B & B & -E \end{bmatrix} \tag{33}$$

where

$$\begin{aligned} A &= 1 - \sin\pi\ell - \cos\pi\ell - 2\sin\frac{\pi\ell}{2} - i\left(1 - \sin\pi\ell + \cos\pi\ell + 2\cos\frac{\pi\ell}{2}\right) \\ B &= 2\left(\cos\pi\ell + \sin\frac{\pi\ell}{2} + \cos\frac{\pi\ell}{2}\right) \\ E &= -2\left(1 - \sin\frac{\pi\ell}{2} + \cos\frac{\pi\ell}{2}\right) \\ C &= -E\left(\cos\pi\ell - i\sin\pi\ell\right) \quad . \end{aligned} \tag{34}$$

The elements of the first row of the matrix (33), A_{1j}, i.e., the coefficients for computing the outgoing wave, were found by applying the Gaussian elimination method to equations (30). The other three rows were obtained from the first row by exploiting the symmetry properties of $H(s_j, x)$, equation (27).

Writing out the expression for e^{ix} from equation (31), we have

$$\lim_{x\to\infty} h_1(x) = e^{ix} = \lim_{x\to\infty}\left\{\sum_{j=1}^{4} A_{1j}\, H(s_j, x)\,/\,C_{s_j}\right\} \quad . \tag{35}$$

Replacing x by $-x$ in equation (35), and using equation (27), we obtain

$$\begin{aligned} e^{-ix} &= \lim_{x\to\infty}\left\{\sum_{j=1}^{4} A_{1j}\, H(s_j, -x)\,/C_{s_j}\right\} \cdot \frac{1}{D} \\ &= \lim_{x\to\infty}\left\{\sum_{j=1}^{4} A_{1j}\, e^{i\pi s_j}\, H(s_j, x)\,/C_{s_j}\right\} \cdot \frac{1}{D} \quad , \end{aligned} \tag{36}$$

so that we have

$$A_{2j} = A_{1j}\, e^{i\pi s_j} \quad . \tag{37a}$$

In a similar manner,replacing x by $\mp ix$ in equation (35),

$$A_{3j} = A_{1j}\, e^{-i\pi s_j/2} \tag{37b}$$

$$A_{4j} = A_{1j}\, e^{i\pi s_j/2} \tag{37c}$$

Note that if $\ell > 2$, $h_1(x)$, $h_2(x)$, $h_3(x)$, and $h_4(x)$ all approach infinity as $x \to 0$, because they each contain $H(s_4, x)$ in their respective linear combinations of $H(s_1, x)$, $H(s_2, x)$, $H(s_3, x)$, and $H(s_4, x)$. In particular, $h_1(x) \sim e^{ix}$ as $x \to \infty$, and $h_1(x) \sim$ constant $\times\, x^{2-\ell}$ as $x \to 0$. We can construct a linear combination of $h_1(x)$ and $h_4(x)$ that is bounded at $x = 0$. And since $h_4(x) \sim e^{-x}$ as $x \to \infty$, this combination is still asymptotically an outgoing wave as $x \to \infty$. Denoting the outgoing wave that is bounded at $x = 0$ by $h_5(x)$, using equation (37c) with $s_j = 2 - \ell$, we have, after some manipulation,

$$h_5(x) = h_1(x) - h_4(x) \cdot A_{14}/A_{44} = h_1(x) + h_4(x)\, e^{i\pi\ell/2}$$

$$= B \cdot \left[(1+i)\, \frac{H_\ell(\ell+3,\, x)}{C_{\ell+3}} + \left(\cos\frac{\pi\ell}{2} - i + i \sin\frac{\pi\ell}{2} \right) \frac{H_\ell(1, x)}{C_1} \right.$$

$$\left. - \left(1 + \sin\frac{\pi\ell}{2} + \cos\frac{\pi\ell}{2} \right) \frac{H_\ell(0, x)}{C_D} \right] \quad , \tag{38}$$

where B is given in equation (34). Note that there is no $H_\ell(2-\ell,\, x)$ term in equation (38).

The solid curves in figure 2 display the real part of the outgoing wave $h_{\ell,1}(x)$ for $\ell = 8.5$, computed from the linear combination of the four series $H_\ell(s_j,\, x)$ given in equations (31)-(34). (This value of ℓ corresponds, according to I, equation (19), to a cone angle of $\theta_0 \cong j_{1,1} \,/\, \left(\ell + \frac{1}{2}\right) = .43$ radians $\equiv 24°$.) The computation was done on a 486 microcomputer in double precision (16 digit accuracy) using a Microsoft Fortran 77 program. The gamma functions were computed using the approximation derived by Lanczos (Press *et al.* 1994). It is seen in figure 2a that the series computation breaks down for $x \gtrsim 32$. The breakdown occurs because we are computing a linear combination of the four functions $H_\ell(s_j,\, x)$, each of which is proportional to $e^x = e^{32} \sim 10^{14}$, to obtain a quantity $h_{\ell,1}(x)$ which is ~ 1. The dashed curve is computed from the asymptotic expansion, using the recursion relation (11). It coincides with the linear combination of the $H_\ell(s_j, x)$ series over the range $2.5 \lesssim x \lesssim 32$ and extends the solution to arbitrarily large x. It breaks down, however, for $x \lesssim 2.5$.

Figure 3 shows the result of the same computation for the function $h_{8.5,5}(x)$, which is finite at $x = 0$, obtained using equation (38), rather than for $h_{8.5,1}(x)$, which is infinite at $x = 0$. At small x the computation using the linear combination of the $H_\ell(s_j,\, x)$ series is accurate, at large x the computation using the asymptotic expansions is accurate, and for a very large intermediate range $2.5 \lesssim x \lesssim 32$, they are both accurate representations of

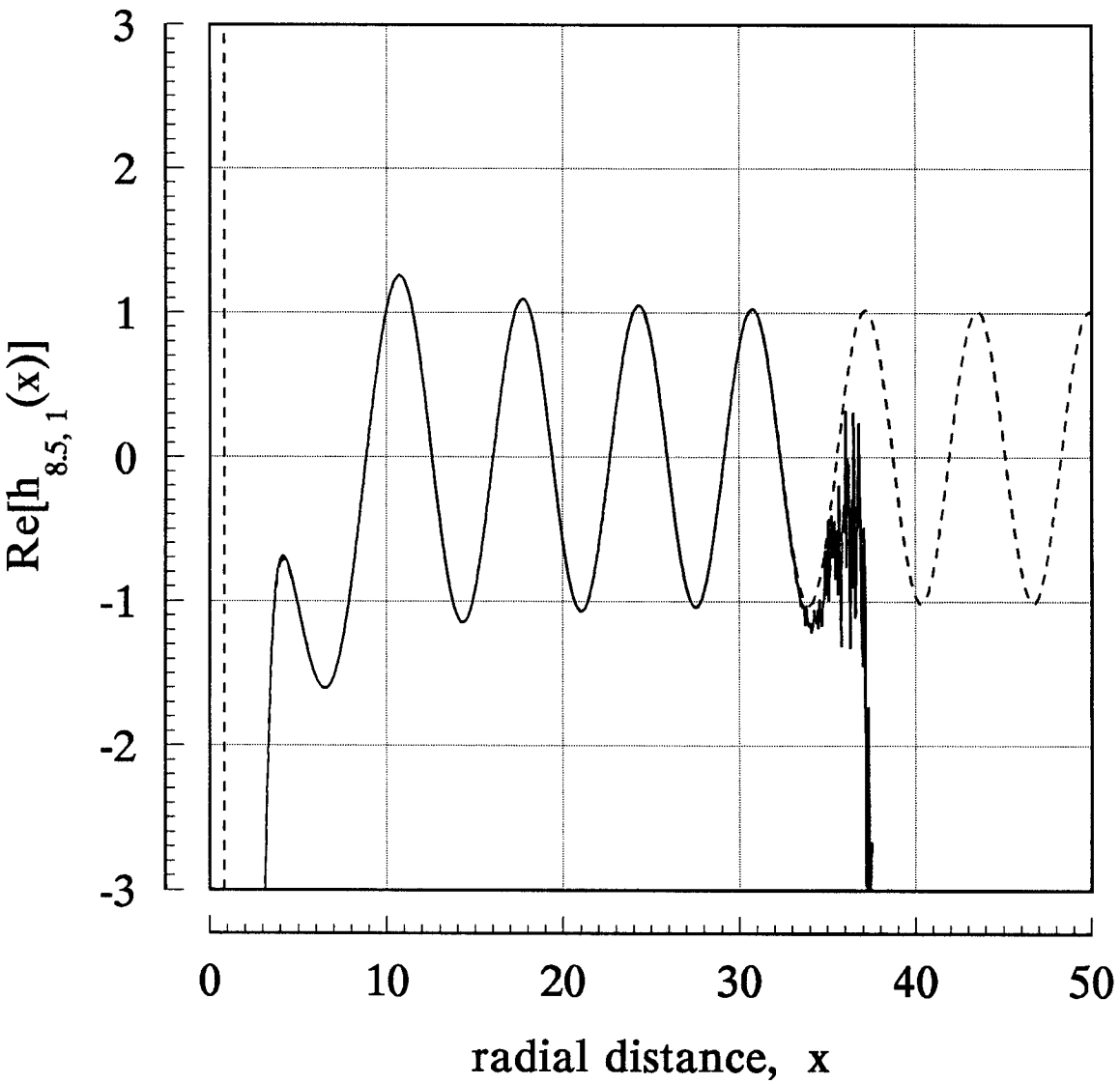

Figure 2: $\mathrm{Re}[\,h_{8.5,1}(x)\,]$ computed using the power series about $x = 0$ (——), and the asymptotic series about $x \to \infty$ (– – – –). **Panel** (a) illustrates the breakdown of the numerical procedure using the power series for $x \gtrsim 32$, and **panel** (b) illustrates the divergence of the asymptotic series from the exact solution for $x \lesssim 2.5$.

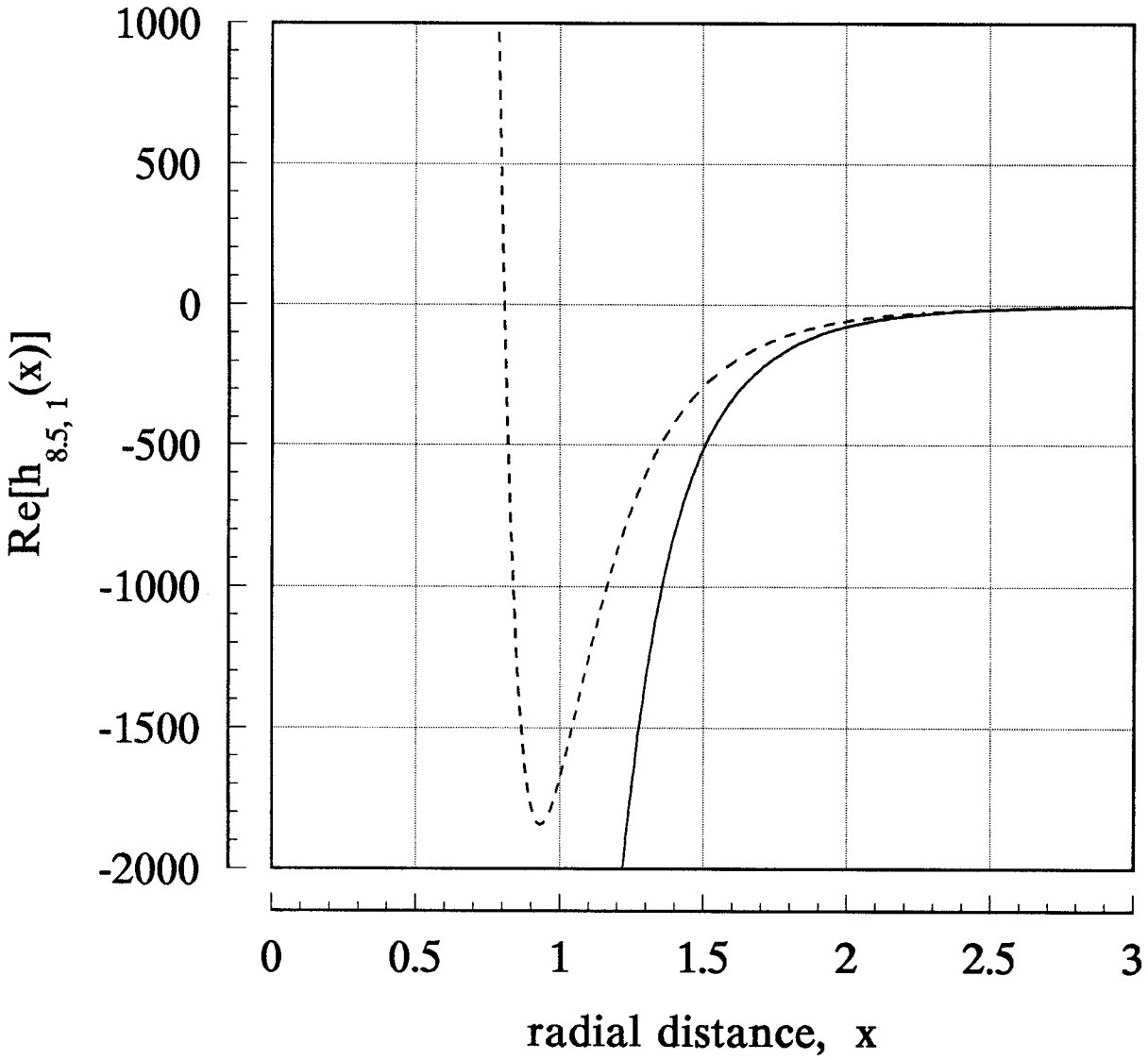
1000
500
0
-500
-1000
-1500
-2000
Re[h 8.5, 1 (x)]
0
0.5
1
1.5
2
2.5
3
radial distance, x

(b)

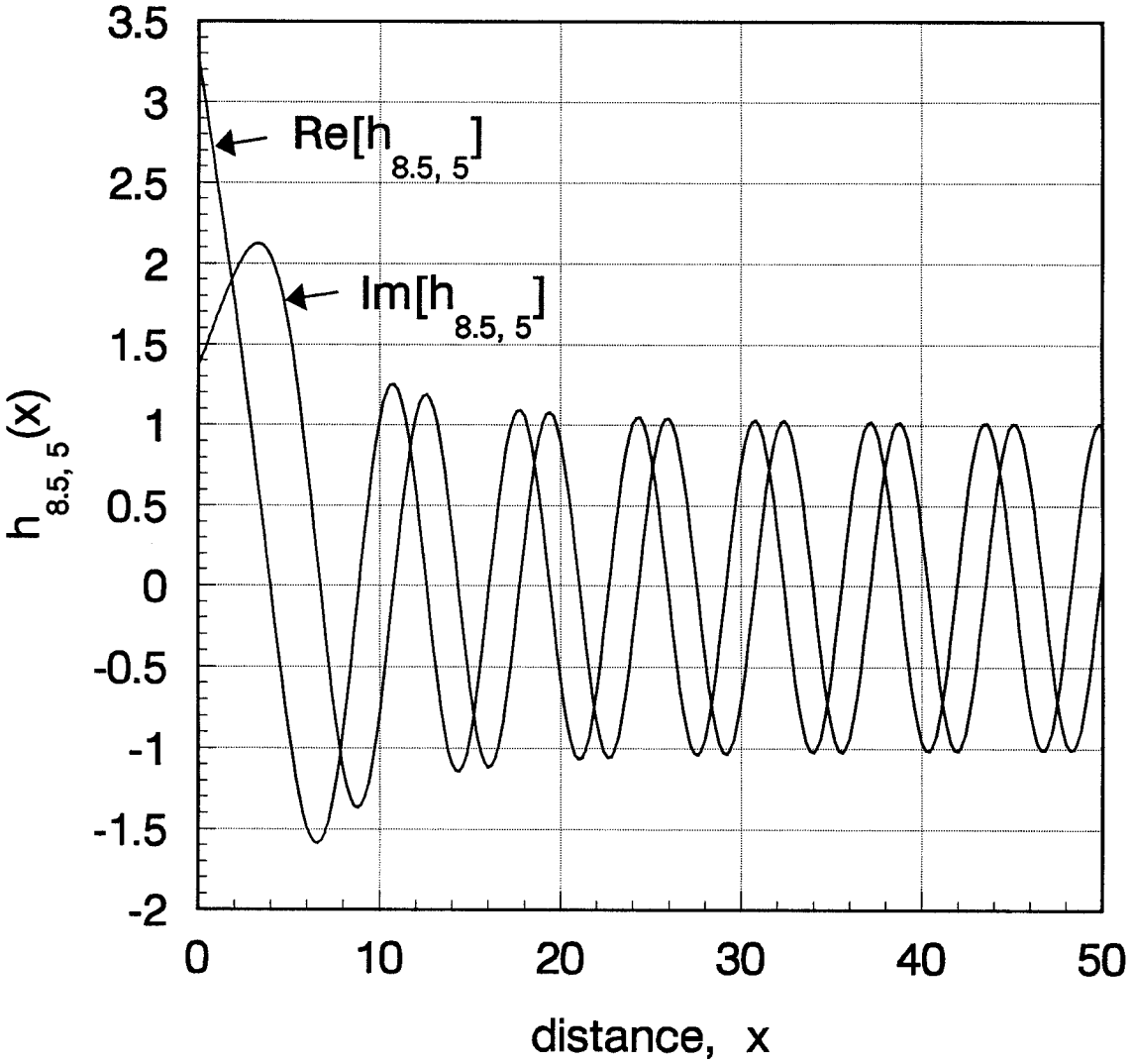

Figure 3: $\mathrm{Re}\,[h_{8.5,5}(x)]$ computed using the power series for $0 \leq x < 20$ and the asymptotic series for $20 \leq x \leq 50$.

the solution. We have illustrated the computations in figures 2 and 3 for $\ell = 8.5$ in order to compare the computation using equations (31-34) and (38) for $\ell = 8.5$ with the computation using equations (9) and (11), shown previously in figure 1d, for the comparable value $\ell = 8$. The results shown in figures 2 and 3 have the same general form as the results for $h_{8,1}(x)$ and $h_{8,5}(x)$ in figure 1d, as one would expect. Below, we will show the dependence on ℓ over a wide range.

It should be noted that, although we have an exact solution in the form of a finite polynomial times an exponential for special values of $\ell = 3, 4, 7, 8, 11, 12, \ldots$, the computation of $h_{\ell,5}(x)$ from these solutions at small x presents computational difficulties. The finite value of these functions $h_{\ell,5}(x)$ at $x = 0$ is the result of a delicate cancellation of large terms in the polynomial-exponential product solutions $h_{\ell,1}$ and $h_{\ell,4}$. Consequently, the linear combination of the four infinite series $H_\ell(s_j, x)$ is the method of choice for computing $h_{\ell,5}(x)$ for large ℓ and small x.

For the most general problem that can be approximated by a sequence of contiguous segments of truncated cones, as described in I, all four solutions $H_\ell(s_j, x)$, $j = 1, 2, 3, 4$, are needed to satisfy boundary conditions between adjacent conical segments (or, equivalently, all four solutions $h_{\ell,j}(x)$). We have not shown the results of numerical computations of the functions $H_\ell(s_j, x)$ because they are not very informative. The oscillations that we have seen in the solutions as a function of x, although obviously present since they emerge after performing the appropriate linear combinations, are totally obscured in the individual $H(s_j, x)$ functions by the exponential growth present in each function.

In figure 4, the real and imaginary parts of the outgoing wave that is finite at $x = 0$, $h_{\ell,5}(x)$ are shown for $0 \leq \ell \leq 28$ and $0 \leq x \leq 30$. The computations were done using the linear combination (38) of the four series $H_\ell(s_j, x)$ for $0 < x \leq 20$ and the asymptotic expansion for $20 < x \leq 30$. We see that for $\ell = 0$, the function settles down to its asymptotic form e^{ix} very quickly. (The solution for $\ell = 0$, is just $h_{0,5}(x) = e^{ix} + e^{-x}$.) For increasing ℓ, it also approaches e^{ix}, but only after oscillation-free intervals of x which increase in length as ℓ increases (much like the behavior of the Bessel function $J_\ell(x)$, for example, except that in the present case the oscillation is undamped). There is a $\pi/2$ phase difference between the oscillation of the real and imaginary parts. In figure 5a and b, the real and imaginary parts of $g_{\ell,5}(x) \equiv d^2 h_{\ell,5}(x) / dx^2$ are shown. According to I, equation (18), $g_{\ell,5}(x)$ is required for calculating the radial component (along the axis of the cone) of the

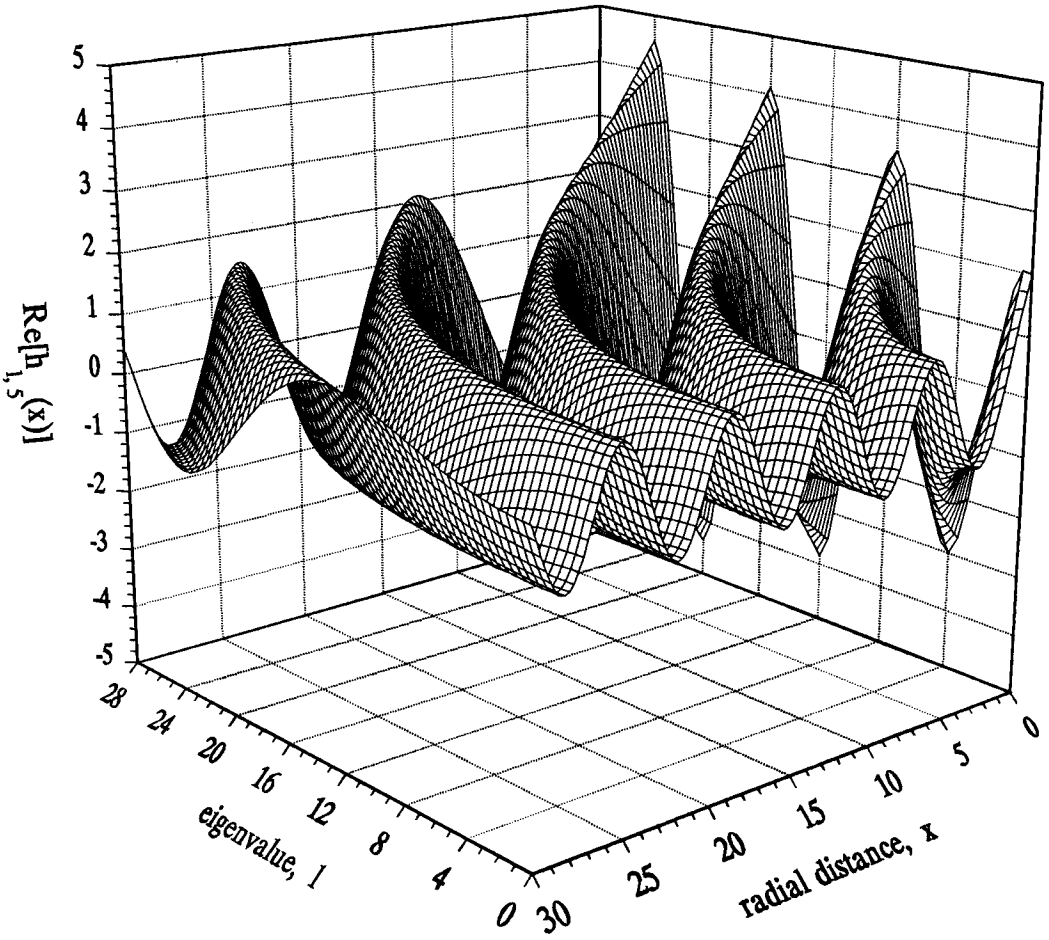

(a)

Figure 4: The real (**a**) and imaginary (**b**) parts of $h_{\ell,5}(x)$, as a function of ℓ and x computed using the power series for $0 < x \leq 10$ and the asymptotic series for $20 < x \leq 28$.

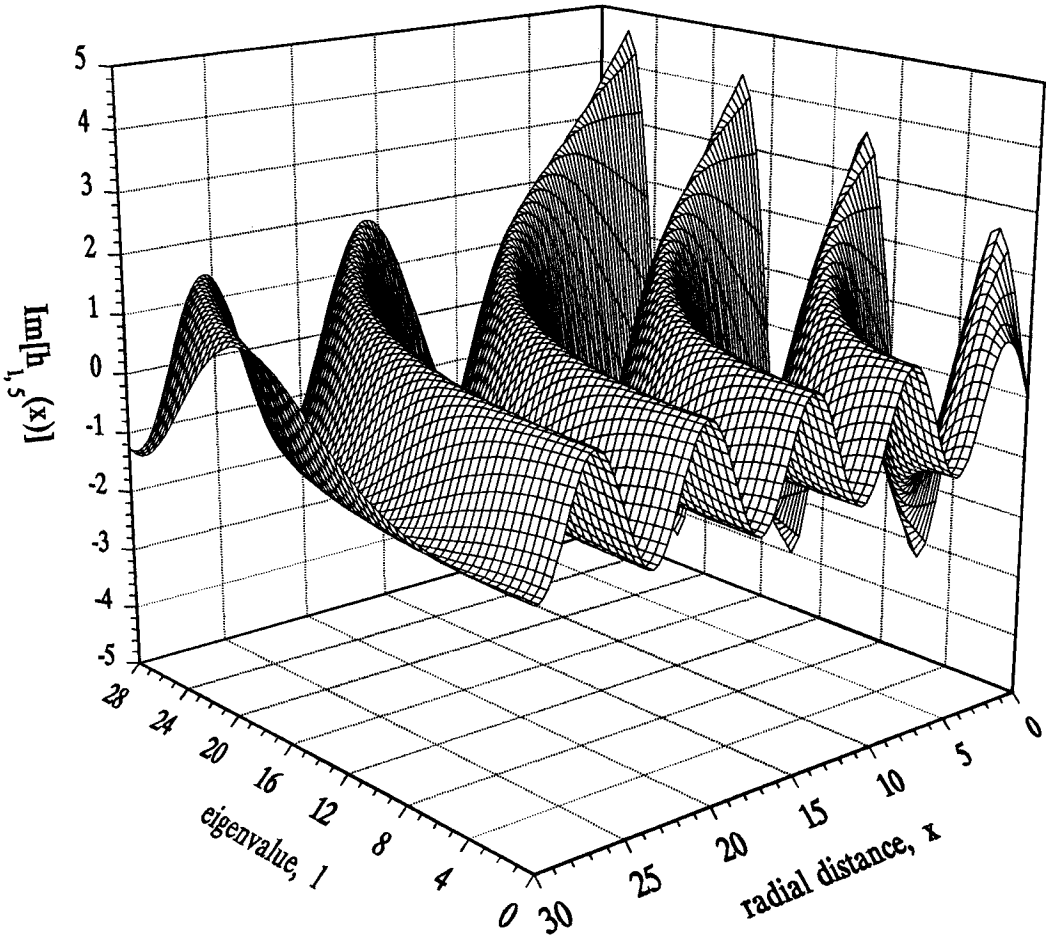
Im[h1,5(x)]
5
4
3
2
1
0
-1
-2
-3
-4
-5
28
24
20
16
12
8
4
0
eigenvalue, l
0
5
10
15
20
25
30
radial distance, x

(b)

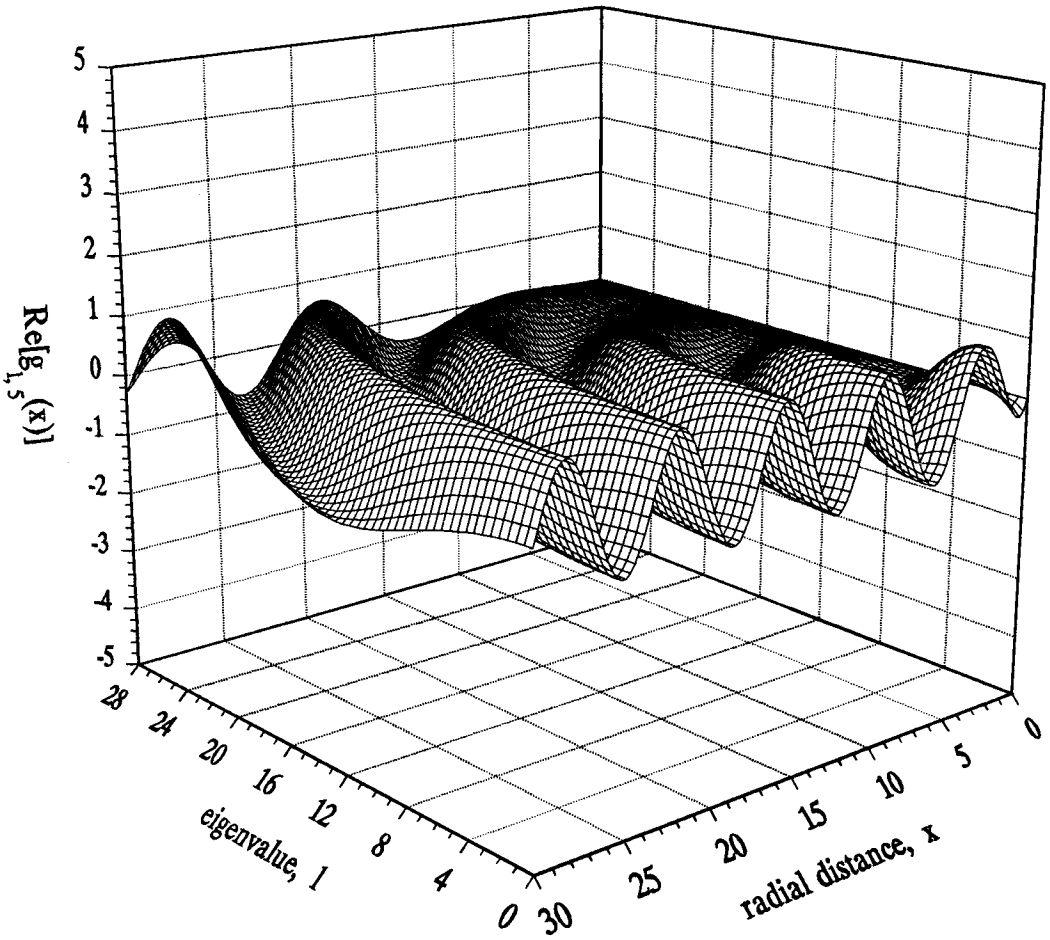

(a)

Figure 5: The real **(a)** and imaginary **(b)** parts of $g_{\ell,5}(x)$ computed as in figure 4.

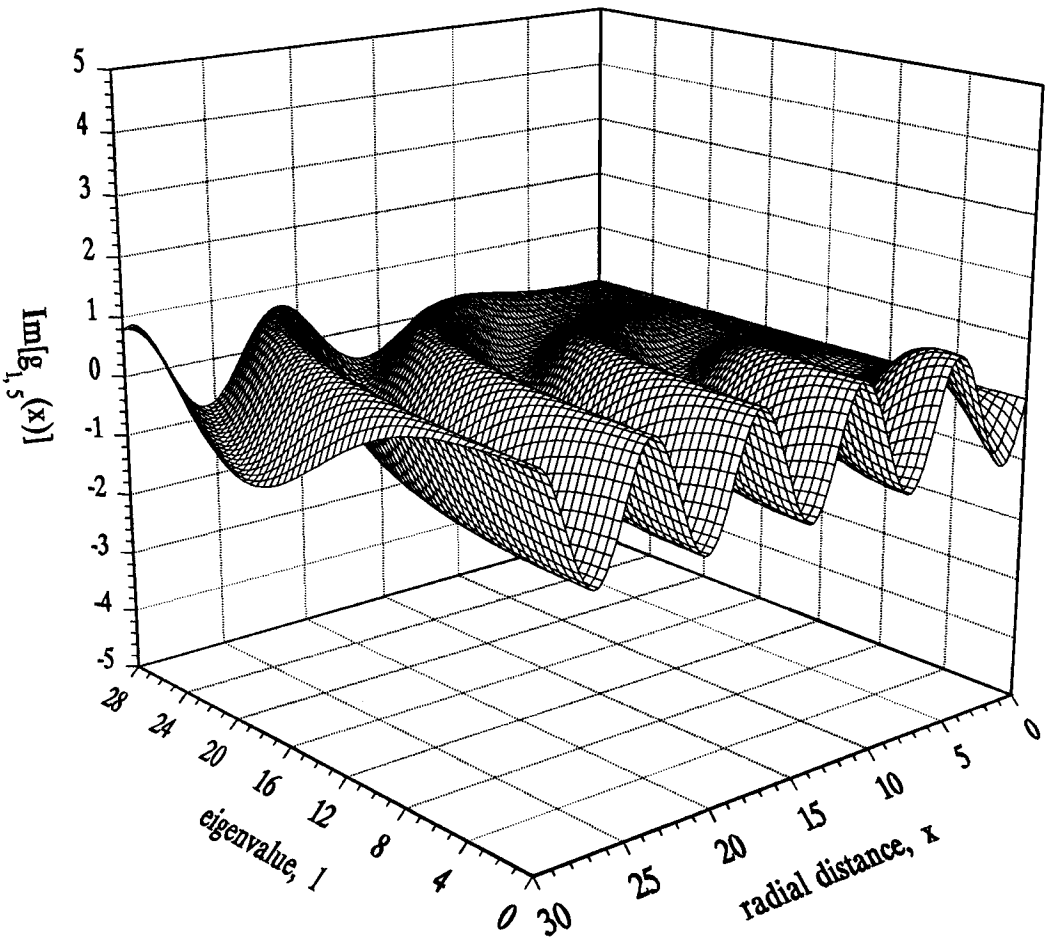
Im[g1,5(x)]
5
4
3
2
1
0
-1
-2
-3
-4
-5
28
24
20
16
12
8
4
0
eigenvalue, l
0
5
10
15
20
25
30
radial distance, x

(b)

magnetic field, and together with $h_{\ell,5}(x)$ for calculating the two components (transverse to the axis) of the electric field.

Acknowledgment

The authors thank Professor F.F. Chen for suggesting this problem and for many helpful discussions.

References

Abramowitz, M. and Stegun, I. A. (1964) "Handbook of Mathematical Functions," U. S. Department of Commerce, National Bureau of Standards, Washington, DC.

Arnush, D. and Peskoff, A. (1995) "Helicon Waves in a Flaring Magnetic Field, Part I: Equations in Spherical Coordinates and WKB-like Wave Solutions".

Dahlquist, G. and Björck, A., translated by Anderson, N. (1974) "Numerical Methods", Prentice-Hall, Englewood cliffs, NJ.

Morse, P. M. and Feshbach, H. (1953) "Methods of Theoretical Physics", McGraw-Hill, New York.

Press, W. H., Flannery, B. P., Teukolsky, S. A., and Vetterling, W. T. (1994) "Numerical Recipes, the Art of Scientific Computing", Cambridge University Press, Cambridge.